Archives Italiennes de Biologie, 149: 426-453, 2011.

Noradrenergic modulation of hypoglossal motoneuron excitability: developmental and putative state-dependent mechanisms

G.D. FUNK[1,2], J.D. ZWICKER[1], R. SELVARATNAM[2], D.M. ROBINSON[2]

[1] Departments of Physiology and Pediatrics, Centre for Neuroscience, Women and Children's Health Research Institute (WCHRI), Faculty of Medicine and Dentistry, University of Alberta, Canada;

[2] Department of Physiology, Faculty of Medicine and Health Science, University of Auckland, New Zealand

ABSTRACT

Hypoglossal (XII) motoneurons (MNs) contribute to diverse behaviors. Their innervation of the genioglossus muscle, a tongue protruder, plays a critical role in maintaining upper airway patency during breathing. Indeed, reduced activity in these MNs is implicated in sleep related disorders of breathing such as obstructive sleep apnea (OSA). The excitability of these MNs is modulated by multiple neurotransmitter systems. The focus of this review is on the modulation of XII MN excitability by norepinephrine (NE), which increases MN excitability through a variety of mechanisms. The level of noradrenergic drive, however, is very dynamic, varying on developmental, sleep-wake and even millisecond timescales relevant to transitions between behaviours. Here we review and provide new data on the maturation of the noradrenergic modulatory system, focusing on those elements specifically relevant to XII MN excitability including the: i) ontogeny of a previously uncharacterized noradrenergic cell group that provides significant noradrenergic innervation to the XII nucleus, the Locus subcoeruleus (LsC); ii) time course over which the XII nucleus is innervated by noradrenergic nerve fibres, and; iii) ontogeny of XII MN sensitivity to NE. We also discuss the hypothesis that the dynamics of MN modulation by NE extend to the spatial domain and present new data suggesting that noradrenergic modulation of the dendritic tree is not uniform but compartmentalized. Implications for information processing are considered. Finally, in the context of state-dependent changes in noradrenergic cell activity, we review mechanisms of NE action most relevant to its role in the muscle atonia of REM sleep.

Key words

XII • Motoneuron • Norepineprhine • Upper airway • REM sleep atonia • Persistent inward current • Locus subcoeruleus

Introduction

Hypoglossal (XII) MNs contribute to a number of rhythmic motor behaviors that are functional from the time of birth including suckling, swallowing, chewing and breathing (Bartlett et al., 1990). Our interest in XII MNs derives primarily from their role in respiration where they mediate tonic and phasic increases in the tone of the genioglossus muscle, a tongue protruder that helps maintain upper airway patency. Their critical role in airway control was emphasized in the mid-70's with the demonstration that reduced muscle tone in the tongue is a significant contributor to obstructive sleep apnea (OSA) (Sauerland and Harper, 1976; Remmers et al., 1978). This observation, combined with the utility of XII MNs for in vitro analysis of basic questions of neuronal excitability and signal processing, make these

Corresponding Author: Gregory D. Funk, 7-50 Medical Sciences Building, Department of Physiology, University of Alberta, Edmonton, Alberta, Canada, T6G 2H7 - Tel.: 1-780-492-8330 - Fax: 1-780-492-8915 - Email: gf@ualberta.ca

neurons among the best characterized in the central nervous system. Intrinsic membrane properties, glutamatergic, glycinergic and GABAergic synaptic properties as well as mechanisms by which multiple neuromodulatory systems (including those that show state-dependent changes in activity) affect information processing have been extensively examined (Berger, 2000; Rekling et al., 2000). The main focus of this article is on the role played by the neuromodulator, norepinephrine (NE), in modulating the activity of XII MNs. The influence of NE on XII MN output changes dramatically during perinatal development (Funk et al., 1994; Kubin and Volgin, 2008) and it is one of the main modulators underlying state-dependent changes in the excitability of XII MNs. Improper development of noradrenergic networks and loss of noradrenergic drive during sleep are also implicated in sleep disordered breathing in infants and adults, OSA (Remmers et al., 1978; Mezzanotte et al., 1992; Fenik et al., 2004; Fenik et al., 2005a; Chan et al., 2006; Horner, 2009), SIDS (Denoroy et al., 1987; Sawaguchi et al., 2003; Hilaire, 2006), Rett Syndrome (RS) (Viemari et al., 2005), and attention deficit hyperactivity disorder (Comings et al., 2000). Discussion will focus specifically on: i) postnatal developmental of the noradrenergic system involved in modulating XII MN excitability with a specific focus on maturation of noradrenergic cells groups, NE innervation of the XII nucleus and XII MN sensitivity to NE; ii) the importance of noradrenergic signaling in mediating the changes in XII MN excitability that occur with transition between sleep-wake states, especially its role in REM sleep atonia, and; iii) implications and evidence for functional compartmentalization of noradrenergic inputs to specific parts of the XII MN dendritic tree. Discussions of serotonergic, cholinergic and peptidergic modulation of XII MN excitability are available elsewhere (Bayliss et al., 1997; Berger, 2000; Rekling et al., 2000; Horner, 2008b, 2009; Dempsey et al., 2010).

Postnatal developmental of the noradrenergic system that modulates XII MN excitability

A complete understanding of the postnatal ontogeny of the noradrenergic system and its potential significance for modulating the excitability of XII MNs requires that it be considered at three levels of organization. These include the developmental time course over which: (i) noradrenergic cell groups innervating the XII nucleus develop the noradrenergic phenotype (i.e. the ability to produce and release NE); (ii) NE-containing neuron terminals innervate the XII nucleus and (iii) XII MNs become sensitive to norepinephrine, which is determined by the developmental expression of NE receptor subtypes, relevant signaling cascades and membrane delimited ion channel effectors.

Ontogeny of noradrenergic cell groups that innervate the XII nucleus

The formaldehyde-induced fluorescence or Falck-Hillarp staining technique (Falck and Torp, 1962) was originally used to identify catecholamine containing cell groups in the brain. However, as this method does not distinguish between the different catecholamines, immunohistochemical techniques utilizing antibodies against specific catecholamine synthesizing enzymes tyrosine hydroxylase (TH), dopamine-β-hydroxylase (DBH) and phenylethanolamine-N-methyltransferase (PNMT) are now widely used to characterize the distribution of dopaminergic, noradrenergic and adrenergic neurons, respectively.

Catacholamine cell groups are distributed throughout the CNS. The brainstem contains three adrenergic (C1-C3), seven noradrenergic (A1-A7) and three dopaminergic cell groups (A8-A10; midbrain) while the forebrain contains seven dopaminergic cell groups (A11-17) (Pearson et al., 1983; Hokfelt et al., 1984; Barnes et al., 1988; Smeets and Gonzalez, 2000). However, the A3 cell group, originally identified in the dorsal aspect of the inferior olivary nucleus (Dahlström and Fuxe, 1964), has not been consistently identified (Smeets and Gonzalez, 2000). In addition, more recent immunohistochemical analyses suggest that the majority of the A2 cell group is dopaminergic or adrenergic but not noradrenergic (Kalia et al., 1985a, 1985b; Smeets and Gonzalez, 2000). The noradrenergic cell groups innervating the XII nucleus include the Locus subcoeruleus (LsC) (a caudo-ventral extension of A6), A7 and A5 cell groups (Aldes et al., 1992). Original reports indicated that the majority (69%) derives from the LsC, while A7 (21%) and A5 groups (10%) make more minor contributions (Aldes et al., 1992).

However, more recent data indicate that neurons of the A7 group have the highest proportion of axonal projections to the XII nucleus (Rukhadze and Kubin, 2007b). Consistent with this, inhibition of the A7 group, but not LsC or A5, reduces spontaneous XII nerve activity in anesthetized rats (Fenik et al., 2008). Thus, LsC may not be the dominant source of input. This question will remain unanswered until the density and specific distribution of NE terminals in the XII nucleus that derive from each cell group is determined.

Despite the fact that TH does not distinguish between dopaminergic, adrenergic or noradrenergic neurons, it has been most widely used to study the development of catacholamine cell groups. Rats and mice are primarily used in these studies due to their short gestation period lasting ~19 and 21 days (E19-E21) respectively. The noradrenergic cells, as detected by TH immunoreactivity, are first evident at E12.5 in rats when neurons are still migrating and distinct cell groups are evident by E13.5. By E18 in rat, distribution and morphology of TH-containing neurons resembles that of the adult (Specht et al., 1981a, b). In humans catacholamine neurons attain adult-like distribution patterns by 14.5 weeks of gestation and adult-like morphology by 25 weeks of gestation (Lorke et al., 2003).

These systems/cell groups, however, are not mature at birth. In fact they do not reach maturity until some time after the second postnatal week (Fukuda et al., 1989; Aldes et al., 1996). The biosynthetic capacity of the catacholamine neurons to produce catecholamines in rat, for example, does not mature until postnatal day 14-21 in rats. TH activity in brainstem catecholamine cell groups, assessed by measuring L-DOPA via high-performance liquid chromatography coupled with electrochemical detection on tissue micro-punched from regions containing A1, A2, A5, A6 and A7 noradrenergic cell groups, increases sharply during the first three days of development and again between P14 and 21 (Roux et al., 2003). Of these groups, changes in A5 and A7 are most relevant in the context of understanding the ontogeny of XII modulation by NE. The third group that provides NE innervation to the XII nucleus has not been examined. We therefore quantified the optical density (O.D.) of TH immunolabeling in the LsC of mice at ages P0, 3, 7, 14, 21 and adult. O.D. is reported relative to levels measured at P0 (Fig 1A, B). O.D. of TH immunolabeling in LsC increased 11.6 ± 2.4% (n = 387 neurons) in LsC between P0 and P3. TH O.D. peaked at P14 at levels that were 29.4 ± 4.7% greater than P0 values (n = 354). TH O.D. remained at these levels at P21 but then decreased by adulthood to levels that were 12.9 ± 5.0% greater that P0 (n = 373); this level of staining was lower than at P14 but significantly higher than at P0.

A limitation of these TH data is that NE synthesis is also dependent on DBH activity. Thus, development of the NE phenotype requires analysis of DBH, or alternatively NE labeling. We therefore quantified the O.D. of NE immunolabeling in the LsC of mice at the same ages as reported for TH (Fig. 2). The O.D. of NE immunolabeling in LsC followed a developmental profile similar to that of TH, but the changes were much more dramatic. NE OD increased 38 ± 9% (n = 376) in LsC, between P0 and P3. The relative O.D. of NE labeling in the LsC cell group continued to increase over the first week and peaked at P7 (104 ± 13%; n = 349) where it plateaued until P14 (94 ± 5%; n = 355). NE O.D. then decreased significantly by P21 (27 ± 8%; n = 316, Fig 2) to levels that remained significantly higher than at birth. In adulthood, the relative O.D. of NE immunolabeling (-19 ± 6%; n = 312) was significantly lower than at birth.

Noradrenergic innervation of the XII nucleus

The XII nucleus contains MNs that innervate a number of functionally distinct tongue muscles. These MNs are somatotopically organized within the nucleus. Of greatest relevance to airway control during breathing are the extrinsic tongue protruders, the largest of which is the genioglossus muscle. Although oversimplified and species differences exist, the general pattern is that genioglossus MNs are located in the ventro-medial aspect of the XII nucleus and innervate the genioglossus muscle via the medial branch of the XII nerve (Krammer et al., 1979; Sokoloff and Deacon, 1992; Sokoloff, 1993; Dobbins and Feldman, 1995). Genioglossus MNs participate in chewing, swallowing and breathing (Bieger, 1991), and there is also some somatotopic separation of genioglossus with respect to specific behaviors. For example, genioglossus MNs located rostral to obex are biased toward involvement in inspiration and those caudal to obex with chewing (Yasuda et al., 2002). The adult pattern is apparent

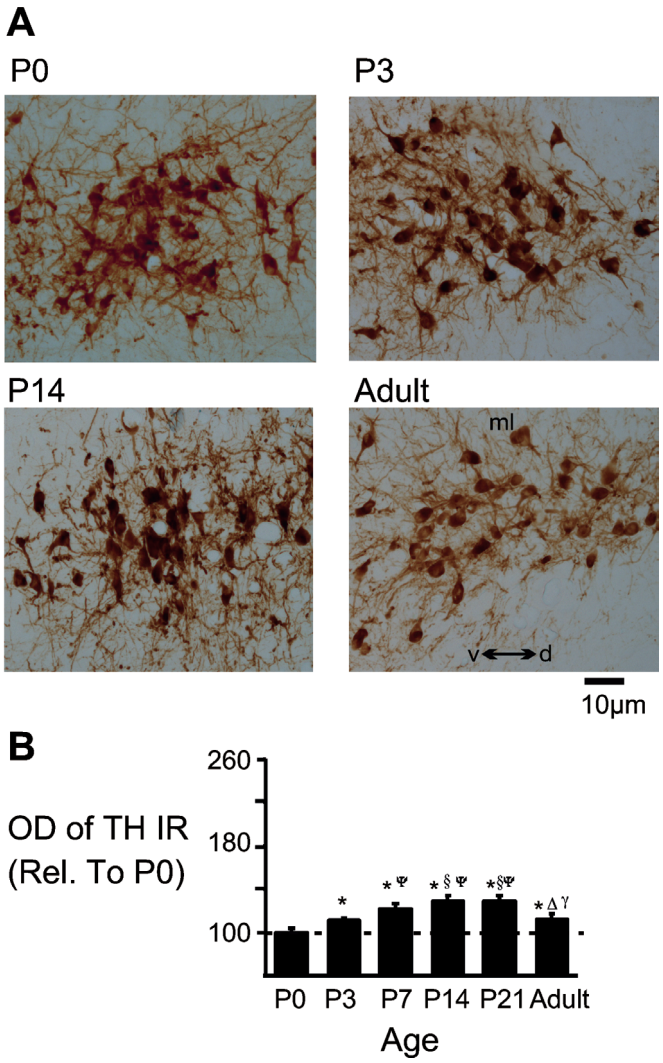

Fig. 1. - Development of TH immunoreactivity in the Locus subCoeruleus. (A) Micrographs, in the transverse plane, of TH immunolabeled LsC neurons of P0, P3, P14 and adult mice (n = 6/age group). The dorsoventral orientation of each image (d - v) and the edge closest to midline (ml) are indicated and are the same in each panel. (B) Histogram of average optical density of cells in the LsC at P0 (n = 367 cells), P3 (n = 342 cells), P7 (n = 387 cells), P14 (n = 354 cells), P21 (n = 345 cells) and Adult (n = 373 cells) relative to the average optical density at P0. The vertical axis extends from 60-260 to cover range of optical densities observed with NE immunoreactivity (Fig. 2). Dashed line indicates optical density of TH labeling at P0 (100%). Vertical bars represent SE; * Optical density values are significantly different from those in P0 mice; Ψ Significantly different from P3 mice; § Significantly different from P7 mice; Δ Significantly different from P14 mice; γ Significantly different from P21 mice.

Methods: All experiments (Figs. 1-8) were approved by the University of Alberta or Auckland animal ethics committees. Experiments were performed on Swiss CD mice of either sex. Males and females were used for all ages except adults, which comprised males only. Day of birth was designated as P0. For detection of TH immunolabeling, mice were anesthetized (n = 36, 6 in each of 6 age groups), and transcardially perfused (4% formaldehyde, 0.5% gluteraldehyde in 0.1 M phosphate buffer). The tissue was cryoprotected by incubation in 10% (12 h) and then 30% (23 h) sucrose solutions. Brainstem tissue was blocked and stored at -80°C until tissue from all age groups was collected. Tissue from all age groups was then cryosectioned (30 μm) and processed simultaneously and identically. Data were only included from experimental runs in which immunolabeling was successful in all age groups, as this was essential to permit comparison between age groups. A single experiment comprised the analysis of sections from all age groups that were processed at the same time under the same conditions. Images of TH (and NE in Fig. 2) immunostaining in LsC were captured using a Leitz Wetzlar (Dialux 20) microscope attached to a CCD video camera and frame grabber (JVC, KY-F450). All images were captured under identical conditions, with aperture size, light intensity and exposure time set manually. Images were imported into NIH Image (v. 1.61), converted into 256 gray scales. The OD of individual neurons was defined as the OD of the cytoplasmic (i.e., non-nuclear) region only minus background O.D. O.D. values are normalized relative to those of the P0 animal within each run. Normalized data for each run (6 animals, 1 from each age) were pooled and averaged. Developmental changes in TH (and NE labeling in Fig. 2) in LsC neurons were assessed using a two-way analysis of variance, followed by a multiple comparison test using SAS 6.1.

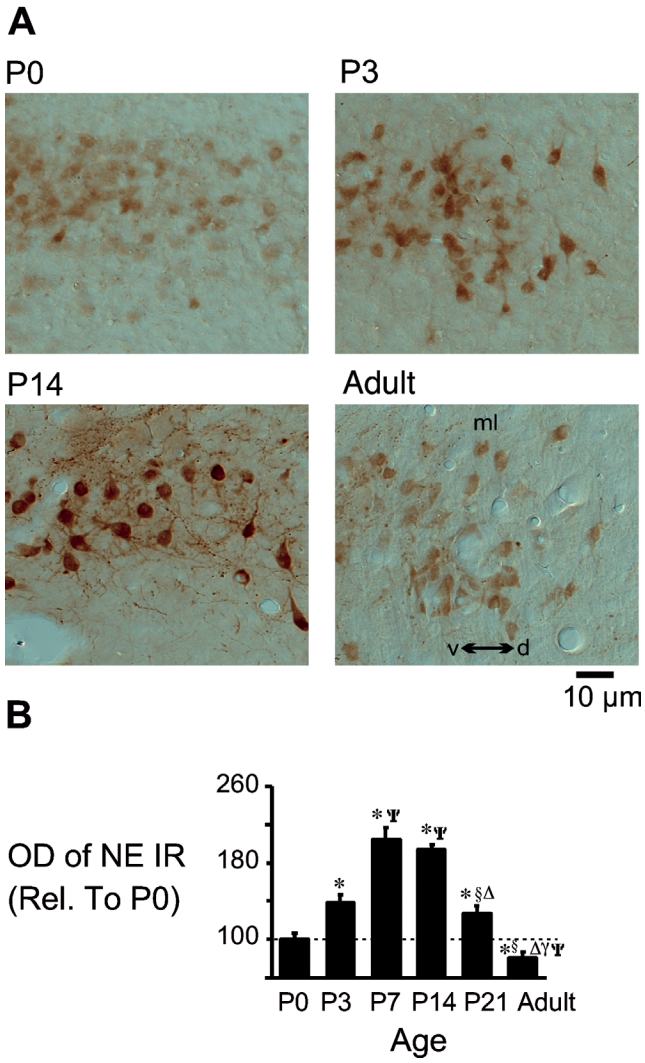

Fig. 2. - Development of NE immunoreactivity in the Locus subCoeruleus. (A) Micrographs of NE immunolabeled LsC neurons of P0, P3, P14, and adult mice. The dorsoventral orientation of each image (d - v) and the edge closest to midline (ml) are the same in each panel. (B) Histogram of average optical density of cells in the LsC at P0 (n = 353 cells, n = 6 animals), P3 (n = 376 cells, n = 6 animals), P7 (n = 349 cells, n = 6 animals), P14 (n = 355 cells, n = 6 animals), P21 (n = 316 cells, n = 6 animals) and adult (n = 312 cells, n = 6 animals) relative to the average optical density at P0. Dashed line indicates optical density of NE labeling at P0 (100%). Vertical bars represent SE; * Optical density values are significantly different from those in P0 mice; Ψ Significantly different from P3 mice; § Significantly different from P7 mice; Δ Significantly different from P14 mice; γ Significantly different from P21 mice. Methods: Tissue collection for detection of NE immunolabeling was similar to that for TH except that mice were perfused with 5% gluteraldehyde before brainstem and spinal cord were removed and post-fixed in PBS solution containing 5% gluteraldehyde. NE immunohistochemistry was performed on every third section through the LsC. Free floating sections were washed in PBS+, incubated in 0.3% H_2O_2 (1 h), 100 µM sodium borohydride (20 min for antigen retrieval), washed in PBS+ (10 min), incubated in 10% sheep serum (1 hr), incubated in the primary antibody (polyclonal rabbit anti-NE, Chemicon International, 1:5000 for LsC and 1:2000 for XII, 5°C, shaken every 12 h). Sections were then washed (PBS+, 3 x 30 min), immersed in biotinylated anti-rabbit IgG (1:400, 24 h), washed (PBS+, 3 x 30 min), incubated in ExtrAvidin-peroxidase conjugate (1:1000, 24 h), and washed (PBS+, 3 x 30 min). Following the DAB reaction, sections were slide-mounted, air-dried and cover-slipped with hystomount. Sections processed concurrently in the absence of primary antibody showed no labeling.

as early as postnatal day 2 (Sokoloff, 1993) and probably earlier since programmed MN cell death is complete prior to birth (Friedland et al., 1995).

Due to the somatotopic organization of the XII nucleus, a full understanding of the functional significance of any modulatory input requires that its distribution be assessed in relation to this somatotopy. TH immunoreactive fibers are first evident in the XII

nucleus at E16 in rats (Aldes et al., 1996). The topographic distribution of catacholamine innervation of the XII nucleus assessed at E19 using TH labeling is reported to be adult-like, with preferential targeting of the ventromedial region of the nucleus (Aldes, 1990; Aldes et al., 1996) that contains genioglossus MNs. However, immunolabeling for NE in the spinal cord varies considerably with respect to both distribution pattern and the density of the innervation during postnatal development (Rajaofetra et al., 1992), suggesting a disparity between identifying NE terminal density with TH *vs*. NE. Our analysis of NE terminal density in the XII nucleus of the postnatal mouse reveals dramatic postnatal changes in NE varicosities. This is illustrated in mice at two time points groups (P3 and P14) by darkfield images showing NE immunolabeling in the ventromedial portion of the XII nucleus at the level of obex (Fig. 3A).

At the first level of analysis, the total number of varicosities counted within the nucleus (from a total of four 30 μm sections, one at each rostrocaudal division of the XII nucleus) was reported per animal to get a global estimate of NE innervation in the different age groups (Fig. 3B, n = 6 animals/age group). At birth, NE-immunolabeled terminals in the XII nucleus were present but sparse (980 ± 200 boutons and 1380 ± 410 μm^2). However, by P3 both the number and area covered by NE-immunolabeled varicosities increased on average to 1620 ± 380 boutons and 2470 ± 800 μm^2 respectively. This increase continued over the first week reaching levels of 3240 ± 360 boutons and 5960 ± 570 μm^2 at P7. Levels peaked by the second week of development when 6190 ± 380 NE labeled terminals, more than 6-fold greater than at P0, occupied an area of 13960 ± 1325 μm^2. After peaking at P14, NE terminals decreased in number to 4970 ± 580 boutons, occupying an area of 10050 ± 1200 μm^2 at P21 and 3430 ± 380 boutons and 7430 ± 1130 μm^2 in the adult. Despite the dramatic fall after P14, levels in the adult were still more than 3 times greater than at P0, and similar to those measured at P7. By adulthood it is clear that innervation patterns are not uniform. The ventromedial, caudal regions of the XII nucleus contains higher numbers of noradrenergic varicosities than any other part of the XII nucleus nucleus (Aldes, 1990; Aldes et al., 1996; Rukhadze et al., 2010). A more detailed developmental analysis of NE terminal innervation patterns along the rostrocaudal and dorsoventral axes of the XII nucleus in relation to its somatotopic organization is required.

Ontogeny of XII motoneuron responsiveness to NE

Ontogeny of noradrenergic receptor subtype expression in XII MNs

NE achieves its signaling actions by binding to a diversity of G-protein coupled receptors that are classified into three main subtypes. α_1 receptors comprise α_{1a}, α_{1b}, and α_{1d} receptors (McCune et al., 1993; Weinberg et al., 1994; Alonso-Llamazares et al., 1995); α_2 receptors subdivide into α_{2a}, α_{2b} and α_{2c} receptors (Zeng et al., 1990; McCune et al., 1993; Rosin et al., 1996; Talley et al., 1996), while β receptors include β_1 and β_2 receptors (Nicholas et al., 1993). All of these are differentially expressed throughout the central nervous system (Nicholas et al., 1996; Day et al., 1997).

Autoradiographic studies report high levels of α_1-noradrenergic receptors in the midbrain and brainstem of new born rats (Jones et al., 1985a,b; Bartolome et al., 1987) that change little over the first week of development, but proliferate over the second week to peak at P15 (Bartolome et al., 1987). The increase in receptor binding is followed by decreases over the third and fourth weeks of postnatal development to reach adult levels, which are lower than in the newborn (Bartolome et al., 1987). α_1-noradrenergic receptor binding (autoradiography) in the XII nucleus appears similar to that in the brainstem. Binding is present at birth and then increases over the first three postnatal weeks (Jones et al., 1985b; Bartolome et al., 1987). Antibodies to the α_1 receptor subtypes are available but there are significant concerns about their selectivity (Jensen et al., 2009). Single-cell reverse transcription-polymerase chain reaction (RT-PCR) analysis of mRNA for all adrenergic receptor subtypes expressed by dissociated XII MNs indicates that the α_{1b} receptor is the predominant subtype (Volgin et al., 2001). Transcripts for α_{1a} and α_{1d} receptors were rarely detected.

Amongst the α_2 receptors, α_{2C} mRNA is rare while α_{2A} mRNA has not been detected in XII MNs (Nicholas et al., 1993; Volgin et al., 2001). However, immunohistochemical studies using subtype selective antibodies against α_{2A} (Talley et al., 1996) and α_{2C} receptors (Rosin et al., 1996) suggest a role for these receptors in the XII nucleus of adult rat, but

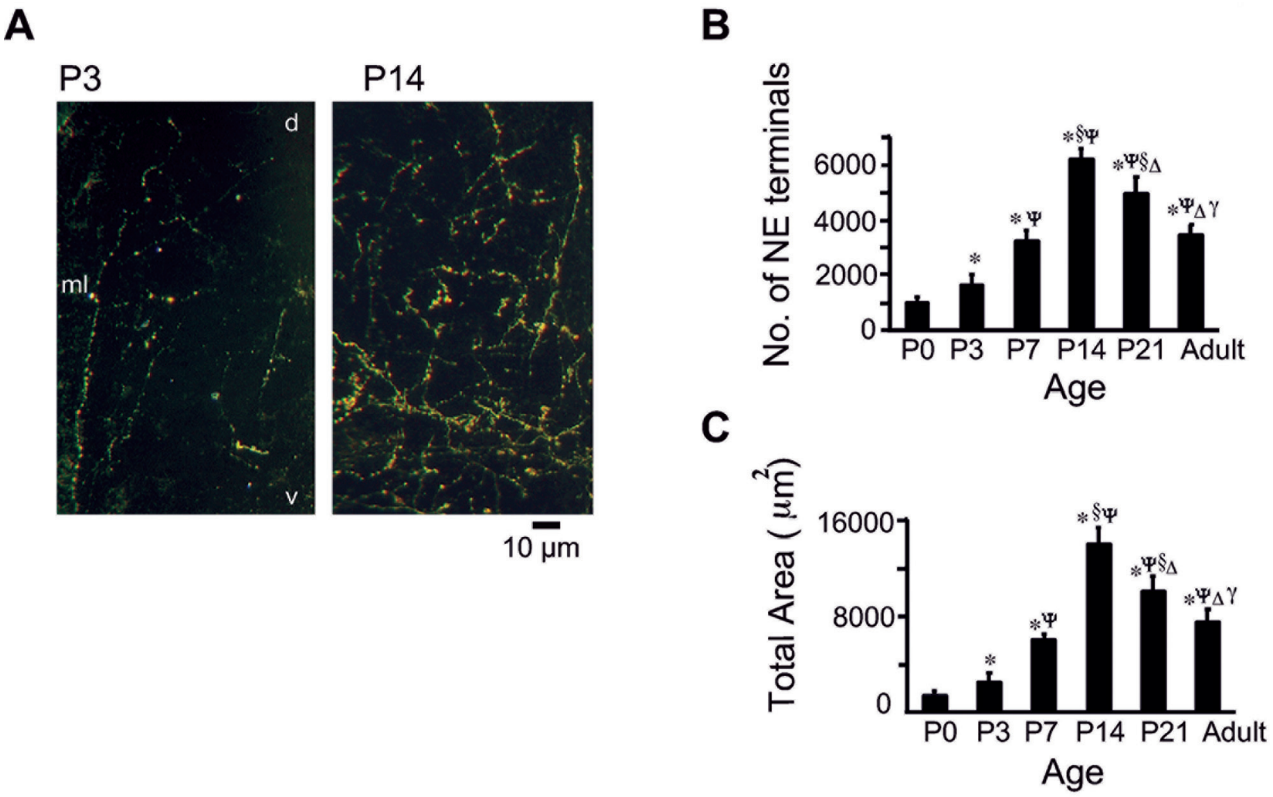

Fig. 3. - Developmental innervation of the XII nucleus by NE immunoreactive fibres. A) Dark field micrographs of NE immunoreactivity in the ventromedial quadrant of the hypoglossal nucleus of P3 and P14 mice. The dorsoventral orientation of each image (d - v) and the edge closest to midline (ml) are the same in each panel. B) Histograms showing average number of NE labeled varicosities (sum of all varicosities at all 4 rostrocaudal levels) and (C) the area occupied by these varicosities in the XII nucleus in P0, P3, P7, P14, P21 and adult mice (n = 6 in each age group). Vertical bars represent SE; * NE labeling values are significantly different from P0 mice; Ψ Significantly different from P3 mice; § Significantly different from P7 mice; Δ Significantly different from P14 mice; γ Significantly different from P21 mice. Methods: Immunolabeling of NE terminals in the XII nucleus was performed as described for LsC neurons (Fig. 2) except that alternate sections were processed and peroxidase staining of NE terminals used a 10-15 min DAB reaction to maximize detection. Images of NE immunolabeled terminals in the XII nucleus were captured (40 x) using a CCD camera (Zeiss Axiocam HRc, 24 bit color) attached to a transmitted light microscope (Axioskop2 Mot Plus, Carl Zeiss, Germany). The XII nucleus extends significantly in the rostrocaudal direction and NE innervation may differ along this axis. The XII nucleus was sub-divided into four rostro-caudal segments (two were caudal to obex, one was at obex and one was rostral to obex) and images taken at all segments. For our initial analysis, labeling at all levels was pooled to quantify total NE innervation within the nucleus. Identical conditions/settings were used between age groups for image acquisition (Image-Pro PLUS). The background labeling varied between age groups, thus different combinations of brightness and contrast values (referred to as the mask) were used for each age group to highlight labeled varicosities. The mask was saved and applied to all images from a specific age group to generate an automated count of the number of NE labeled boutons and a measure of the area occupied by these structures. Manual counts of varicosities, performed in 3 complete developmental runs, were virtually identical to automated counts, verifying the accuracy of the automated process. Statistical analysis of developmental changes in NE terminal labeling involved comparing both the number of NE-containing boutons and area occupied by NE labeling using 6 x 4 x 4 factorial model in log-linear scale to account for heteroscedascity using the statistical analysis package R 2.1.0 (R Foundation, from http://www.r-project.org). The multi-factorial ANOVA was followed by a multiple comparison test to identify differences. Values of $P < 0.05$ were assumed significant.

development analysis is incomplete. The α_2-adrenergic receptor is present in brainstem of human fetuses in mid-gestation, but receptor density decreases during fetal development (Mansouri et al., 2001; Happe et al., 2004). Significant α_2 receptor density remains at birth and levels appear to increase over the first five postnatal days before deceasing to adult levels similar to those at birth (Happe et al., 2004).

Original autoradiographic studies suggested β receptor expression (Rainbow et al., 1984) in XII

MNs, but these data are constrained by ligand binding specificity. Immunohistochemical studies with subtype selective β receptor antibodies (Tohyama et al., 1989) also suggest β receptor expression in XII nucleus of adult rat, but single XII MN RT-PCR analysis did not detect β_1 or β_2 mRNA (Nicholas et al., 1993; Volgin et al., 2001).

Ontogeny of noradrenergic modulation of XII motoneuron inspiratory output and underlying mechanisms

The sensitivity of XII MNs to NE was assessed in Swiss CD mice at P0, 3, 14, 21 and P45-55 (adult). Currents are reported as peak currents (pA) and current densities (pA/pF) to control for developmental increases in MN size. NE evoked inward currents in all MNs tested, but sensitivity changed dramatically during development. As shown for individual MNs (Fig. 4A) and group data (Fig. 4B), peak currents and current densities increased significantly over the first two weeks, plateaued between P14 and P21 and then declined significantly in adulthood (refer to the Fig. 4 caption for details of the statistical analysis). At P0, inward NE currents averaged 42.8 ± 4.4 pA or 2.4 ± 0.3 pA/pF (n = 14). After just three days, NE currents averaged 81 ± 11 pA or 3.0 ± 0.4 pA/pF (n = 17), which represents increases of ~80% and 25% over P0 values, respectively. NE currents increased continually between P3 and 14 reaching values of 147 ± 27 pA (n = 6) or 4.0 ± 0.7 pA/pF at P14 which is an ~80% and 33% increase compared to P3. Currents were similar at P21 (132.4 ± 10.8 pA; 4.0 ± 0.2 pA/pF; n = 6), but decreased significantly by adulthood where they averaged 81 ± 16 pA and 1.63 ± 0.7pA/pF. As expected based on previous analysis of juvenile rat XII MNs (Parkis et al., 1995), NE currents in mouse MNs were associated with significant changes in neuronal input resistance (R_N) that paralleled developmental changes in current magnitude. Baseline R_N values fell significantly during development from 186 ± 27 (n = 11) MΩ at P0, to 149 ± 13 MΩ (n = 12), 92 ± 6 MΩ (n = 6), 86 ± 10 MΩ (n = 6), and 68 ± 5 MΩ (n = 5) at P3, P14, P21 and adult, respectively. At P0 NE induced a significant 5.7 ± 3.3% (n = 8) increase in R_N. This effect increased at P3 (14.0 ± 3.6%, n = 12), peaked at P14 (61.7 ± 9.9%, n = 7) and then declined at P21 (39.0 ± 2.6%, n = 6) and adult stages (16.9 ± 5.5%, n = 5).

The increase in XII MN sensitivity to NE over the first two weeks is associated with a 9-fold potentiation of XII MN inspiratory output (by exogenous NE) (Funk et al., 1993; Selvaratnam et al., 1998), reflecting an interaction between two different receptor mechanisms. The predominant α_1 receptor-mediated, postsynaptic potentiation increases postnatally and is complimented by a small β receptor mediated potentiation. The α_1 potentiating effects reflect at least two main actions. First, α_1 receptor activation potentiates glutamatergic inspiratory synaptic currents. The underlying mechanism is not fully characterized but likely involves activation of protein kinase C (PKC). α_1-adrenergic receptors are classically considered to couple to the $G_{q/11}$-protein (Wu et al., 1992; Wise et al., 1995), which initiate a signal cascade by activating phospholipase C (PLC)-induced hydrolysis of phosphatidyinositol-4,5-biphosphate (PIP_2), which in turn generates the second messengers inositol-(1,4,5)-trisphosphate (IP_3) and diacyl-glycerol (DAG). The IP_3 triggers the release of intracellular Ca^{2+}, which together with DAG activates protein kinase C (PKC) (Zhong and Minneman, 1999), which in turn may phosphorylate AMPA receptors that mediate inspiratory drive. PKC-dependent potentiation of XII MN inspiratory synaptic currents has not been directly demonstrated, but the potentiation of AMPA currents in XII MNs that occurs following intermittent α_1 receptor activation does depend on PKC signaling (Feldman et al., 2005; Neverova et al., 2007).

α_1 receptor mediated potentiation of inspiratory synaptic currents may also reflect noradrenergic potentiation of persistent inward currents (PICs). PICs are voltage- or ion-gated channels that do not inactivate (or inactivate very slowly) once activated. By depolarizing dendritic membrane or locally elevating the concentration of a specific ion (e.g. Ca^{2+}), synaptic inputs can activate PICs that in turn amplify the synaptic input. The majority of spinal MNs in mouse and turtle express a significant dendritic PIC that is primarily mediated by the L-type Ca^{2+} channel. The PICs in mouse spinal MNs are markedly potentiated by aminergic inputs, including NE. In fact, without monoamines, PICs are essentially absent and spinal MN gain is extremely low. This is evident following aminergic antagonism or acute spinal transection, when MN excitability is so low that reflexes are almost absent (Miller et al., 1996; Rekling et al., 2000; Bennett et al., 2001). Whether similar mechanisms occur in XII MNs is not known. XII MNs do

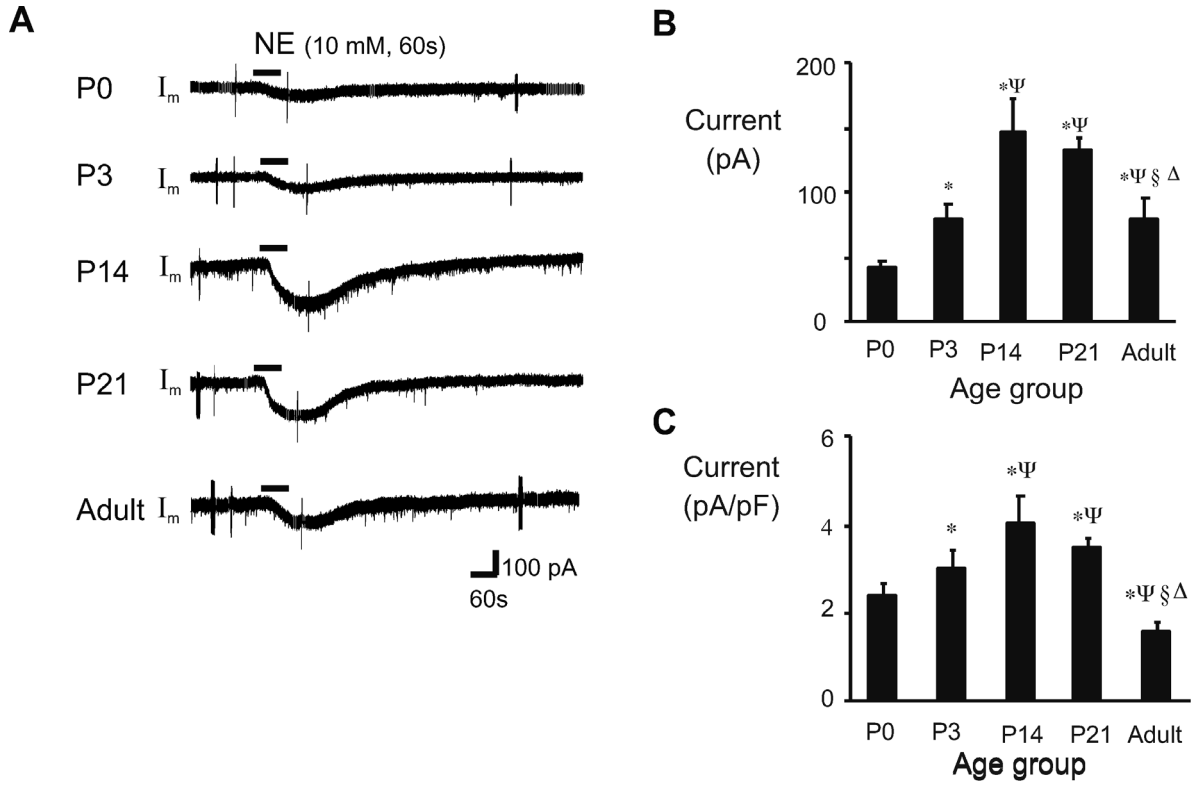

Fig. 4. - NE-induced inward currents in XII motoneurons increase with postnatal development.
A) Whole-cell recordings of membrane currents (Im) evoked by 60 s bath application of NE (10 μM) in XII MNs from brainstem slices isolated from Swiss CD mice of different ages. Bath application was used rather than local application to ensure consistency of NE concentration between age groups. Histograms showing pooled data of absolute NE currents (B) and NE currents reported relative to membrane capacitance (C) in XII MNs during development. Developmental changes in NE currents or current-densities were assessed via analysis of variance, followed by a multiple comparison test using SAS 6.1. Vertical bars represent SE; * Significantly different from P0 mice; Ψ Significantly different from P3 mice; § Significantly different from P14 mice; Δ Significantly different from P21 mice.

express a PIC (Powers and Binder, 2003; Moritz et al., 2007) that has a large dendritic component, but the incidence is reduced relative to spinal MNs and the components of the PIC are different. Whereas the L-type Ca^{2+} channel is the main contributor to the spinal MN PIC, the majority of the persistent current in juvenile XII MNs is carried by N- and P-type Ca^{2+} channels, with only a small contribution from L-type Ca^{2+} channels, and the persistent sodium current, I_{NaP} (Powers and Binder, 2003; Moritz et al., 2007). Whether these currents in XII MNs are potentiated by monoamines is not known. We provide preliminary evidence of a third contributor to the PIC in XII MNs, a Ca^{2+} activated, non-selective cation conductance, I_{CAN}, that is believed to be mediated by the TRPm4 channel (Nilius et al., 2008). I_{CAN} amplifies glutamatergic inspiratory synaptic currents in pre-Bötzinger complex inspiratory neurons up to 5-fold (Pace et al., 2007; Mironov, 2008; Pace and Del Negro, 2008). In inspiratory XII MNs, an α_1 noradrenergic potentiation of glutamate currents appears to be mediated in part through potentiation of I_{CAN} because it is blocked by flufenamic acid (Fig. 5, n = 3). The slow phenylephrine (α_1 agonist) current is not affected by flufenamic acid, but its ability to potentiate glutamate inputs is abolished. Note that the reduction of the glutamate currents by flufenamic acid is not due to nonselective antagonism of NMDA receptors, because flufenamic acid alone does not affect glutamate responses (Fig. 5C). In addition, real-time analysis of mRNA extracted from XII punches and laser capture microdissected XII MNs shows a strong signal for TRPm4, which is believed to mediate the I_{CAN} current (Fig. 6). Note that pre-Bötzinger Complex punches, which contain neurons with a demonstrated I_{CAN}-mediated

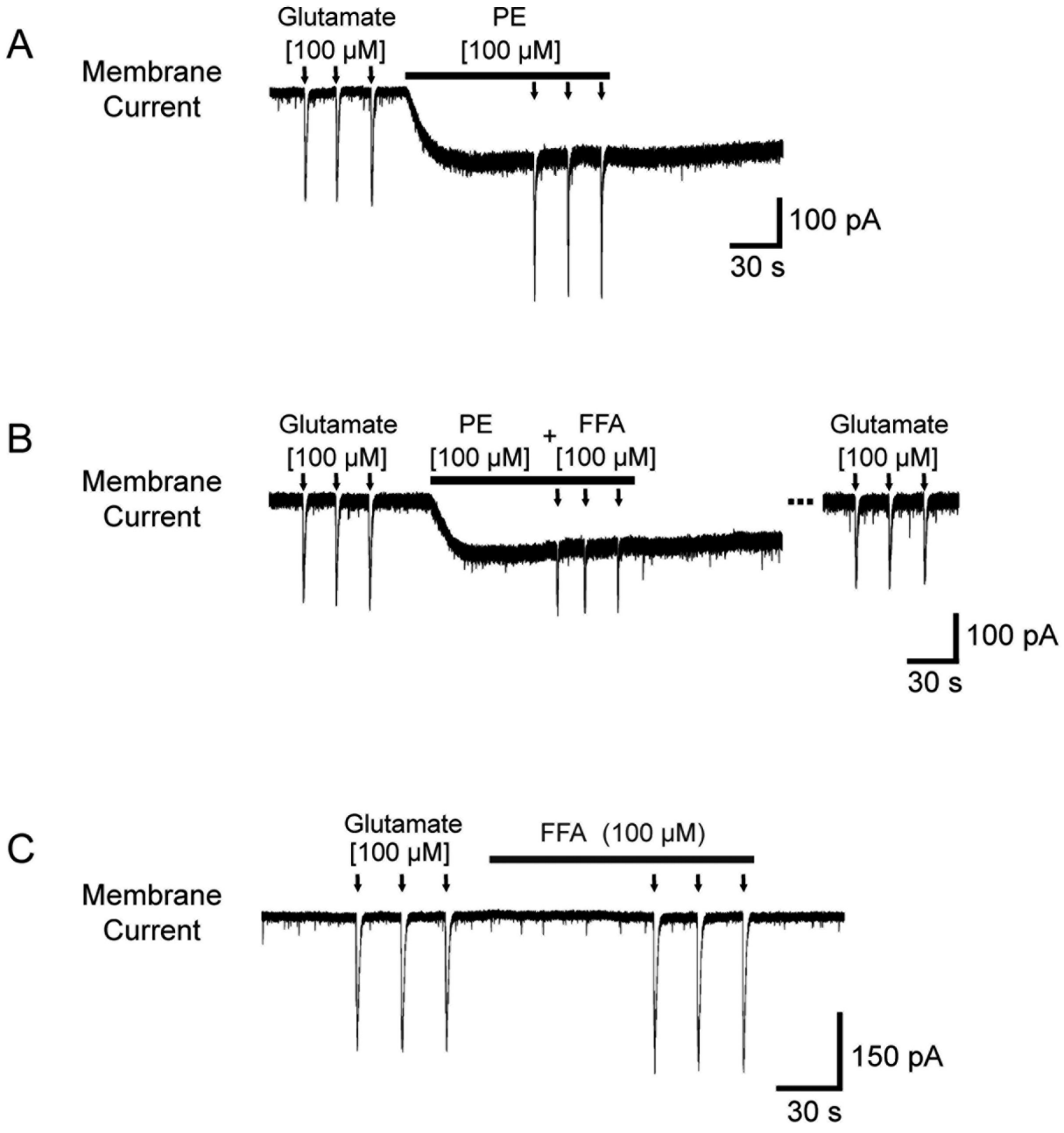

Fig. 5. - Potentiation of glutamate currents in XII motoneurons by the PIC, I_{CAN}. Whole-cell voltage-clamp recording from an inspiratory XII MN in a rhythmic slice from neonatal rat after block of rhythm with TTX. A) Glutamate currents (arrows) are increased in phenylephrine (PE, α_1 noradrenergic receptor agonist). B) In flufenamic acid (FFA, which blocks the PIC, I_{CAN}) glutamate currents are not potentiated by PE. A and B are from the same cell, 15 min apart. C) Different cell; FFA has no effect on glutamate currents.

PIC, also have a significant TRPm4 signal (Pace et al., 2007; Mironov, 2008; Pace and Del Negro, 2008). These data support the hypothesis that amine-sensitive PICs are important in maintaining XII MN excitability to synaptic input, and that PIC reduction during REM sleep will reduce excitability. However, a more thorough analysis of this putative I_{CAN} contribution and its amine sensitivity is required in XII MNs since flufenamic acid, while reportedly selective for I_{CAN} at the concentration used (100 µM), does have nonselective actions. Also, preliminary XII MN data showing that PIC-mediated tail

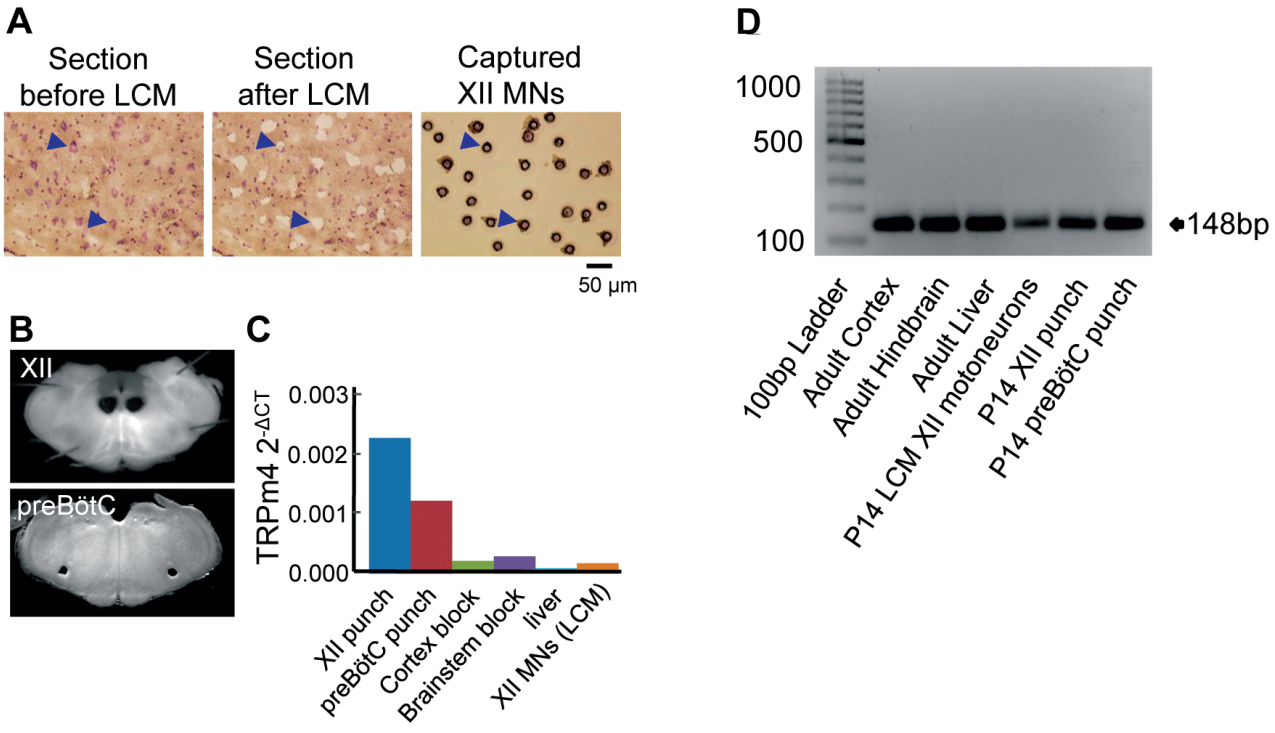

Fig. 6. - XII motoneurons express the transcript for TRPm4, which codes for I_{CAN}. A) Phototriad showing the XII nucleus in a stained tissue section (6 µm) before and after laser capture microdissection (Arcturus AutoPIX II) of XII MNs. The image on the right is of captured neurons. B) 300 µm thick tissue sections after removal of tissue punches from the hypoglossal nuclei (XII) and pre-Bötzinger complex (preBötC) and XII nuclei. C) mRNA extracted from punches, laser captured XII MNs and multiple control tissues was subject to real-time RT-PCR analysis for the TRPm4 transcript. Expression levels are reported relative to cyclophilin A (ΔCT = cycle threshold number for TRPm4 - cycle threshold number for cyclophilin A). D) Gel of real time PCR product showing TRPm4 in various tissue samples. (The TRPm4 forward primer code was 5′-AGTTGAGTTCCCCCTGGACT-3′ and the reverse primer code was 5′-AATTCCAGTCCCTCCCACTC-3′, which generated an amplicon of 148 base pairs).

currents evoked by depolarizing pulses are insensitive to extracellular Na^+ concentration (Powers and Binder, 2003) questions a contribution of I_{CAN}.

The second major mechanism underlying the α_1 noradrenergic receptor potentiation of XII inspiratory MN output is the inhibition of a resting K^+ leak current ($I_{K\ leak}$) (Parkis et al., 1995) that is both barium- and pH-sensitive, and most likely mediated by heterodimers of the two-pore domain potassium channels TASK-1 and TASK-3 (Parkis et al., 1995; Talley et al., 2000; Berg et al., 2004). This current, upon which multiple modulators converge (including substance P (SP)), appears to increase its expression several-fold over the first two postnatal weeks (Adachi et al., 2010). Its inhibition not only depolarizes the membrane, it increases neuronal input resistance such that the inspiratory-evoked depolarization is greater in the presence of NE. The transduction pathway via which α_1 noradrenergic receptors modulate the TASK channels appears to occur via a $G_{\alpha q}$-linked receptor mechanism that is independent of the classical PLC-mediated PIP2 hydrolysis. Instead, it appears that TASK channels, or closely associated intermediaries, are direct effectors for activated $G_{\alpha q}$ subunits (Chen et al., 2006). A second, significant, barium-insensitive component of the α_1 receptor current is mediated by the activation of an as yet unidentified sodium conductance (Parkis et al., 1995).

NE, via α_1 receptors, also reduces the amplitude of the medium afterhyperpolarization (mAHP) in juvenile XII MNs. The mAHP, which follows the action potential, is mediated by a slow Ca^+-mediated K^+ conductance (Nunez-Abades et al., 1993; Berger et al., 1995) and is an important determinant of firing behavior. A larger amplitude, longer dura-

tion mAHP is correlated with lower firing rate of neurons (Walton and Fulton, 1986). Developmental changes in the amplitude of the mAHP are inconsistent (Nunez-Abades et al., 1993; Viana et al., 1994, 1995). However, studies consistently report a developmental decrease in mAHP duration (Nunez-Abades et al., 1993; Viana et al., 1994; Berger et al., 1995; Viana et al., 1995), possibly reflecting a developmental decrease in the low-voltage-activated (LVA) Ca^{2+} current (Berger et al., 1995), which is the main source of Ca^{2+} that activates the Ca^{2+}-induced K^+ conductance (Nunez-Abades et al., 1993; Viana et al., 1993; Berger et al., 1995). However, the LVA Ca^{2+} current in XII MNs of rat does not appear to change over the first few weeks of development (Miles et al., 2004). Thus, the mechanism(s) underlying the developmental decrease in mAHP needs to be revisited. While the efficacy of NE in modulating the mAHP during development is not known, the reduction in the mAHP combined with the α_1-receptor mediated increase in R_N (which do increase postnatally), will increase the slope and cause a leftward shift, respectively, in the relationship between current and the discharge frequency of action potentials (Parkis et al., 1995), both of which will enhance XII MN responses to inspiratory synaptic input.

A putative α_2-receptor mediated inhibition of XII MN inspiratory activity has been reported (Selvaratnam et al., 1998) that may reflect inhibition of the hyperpolarization activated inward current, I_h (Parkis et al., 1997). However, the α_2-receptor agonists used to delineate this mechanism do not discriminate between imidazoline and α_2-receptors. In addition, a careful dose response analysis of clonidine's (α_2 receptor agonist) action on XII MNs convincingly demonstrates, at least in neonatal MNs, that clonidine has no effect on I_h (Adachi et al., 2005). Thus, modulation of XII MN activity by an α_2-receptor mechanism appears unlikely. An α_2-receptor mediated inhibition of I_h in more mature animals, however, can not be excluded because there is an approximate 10-fold increase in I_h current density between neonates and adults (Bayliss et al., 1994; Berger et al., 1995). A role for β-receptors in potentiating the inspiratory output of XII MNs remains possible (Selvaratnam et al., 1998), but RT-PCR analysis questions expression of β noradrenergic receptors in the XII nucleus (Volgin et al., 2001).

Functional Implications of postnatal changes in the noradrenergic system

The data presented and reviewed here indicate a highly coordinated maturation of the noradrenergic system that modulates XII MN excitability. XII MN sensitivity to NE, expression of catecholamine synthesizing enzymes and NE in noradrenergic neurons that project to the XII nucleus, and the innervation of the XII nucleus by NE fibres all increase over the first two postnatal weeks, plateau (or decrease) between P14 and 21 and then decrease into adulthood.

The physiological significance of this developmental profile is not completely known, but consideration of the MNs properties offers some insight. Like noradrenergic (Aldes et al., 1996) and other modulatory systems (Kubin and Volgin, 2008), XII MNs are not mature at birth. Their morphology (Nunez-Abades et al., 1994; Nunez-Abades and Cameron, 1995, 1997), passive and active membrane properties all change significantly during postnatal development (Nunez-Abades et al., 1993; Berger et al., 1996; Rekling et al., 2000). A major consequence is an overall reduction in MN excitability, reflecting increased MN size, but more significantly an increase in resting membrane conductance (decrease in R_N), that comprises an increased expression of background potassium leak conductance (most likely TASK-1/TASK-3 potassium channels) (Nunez-Abades et al., 1993; Viana et al., 1994; Berger et al., 1995; Cameron et al., 2000; Talley et al., 2000; Berg et al., 2004) as well as a 10-fold increase in I_h (Bayliss et al., 1994; Berger et al., 1995). This developmental reduction in excitability is apparent as at least a two-fold increase in the rheobase current, defined as the current strength at which MNs reached firing threshold in one half of the trials, between newborn and adult (Viana et al., 1994; Berger et al., 1995).

In this context, development of the NE system is likely to have important consequences for inspiratory control of the airway because at birth, XII MNs are very excitable and therefore likely to discharge simply in response to glutamatergic inspiratory drive. However, as they mature, reductions in excitability could lead to reduced muscle activity and airway instability. NE has little effect on XII MNs or XII inspiratory activity at birth but its efficacy increases substantially with development; the potentiation of inspiratory drive by exogenous NE increases 9-fold between P0 and P14 (Funk et al.,

1994; Kubin and Volgin, 2008). Development of the NE system may offset developmental reductions in intrinsic MN excitability to maintain MN responsiveness (Bayliss et al., 1994), and in the case of breathing, help stabilize the airway.

In a broader context, XII MNs participate in many behaviours, the profile of which changes postnatally. For example breathing, suckling and swallowing are prominent in the newborn. Through development, suckling decreases while chewing increases. Noradrenergic modulation may enhance XII MN excitability to all types of inputs. However, given the complexity of the MN dendritic tree and the potential for differential distribution of functional and modulatory inputs (see Section *Functional compartmentalization of the dendritic tree*), it is also possible that noradrenergic actions differ between classes of inputs.

Role of NE in the state-dependent modulation of XII MN excitability and REM atonia

The neurochemical control of MN excitability changes dramatically during sleep due to state-dependent increases in activity of cholinergic pontine neurons (el Mansari et al., 1989; Steriade et al., 1990) and glycinergic/GABAergic neurons (Yamuy et al., 1999; Engelhardt et al., 2004), and decreases in activity of serotonergic raphe neurons (Jacobs and Fornal, 1991; Leung and Mason, 1999) and noradrenergic neurons (Aston-Jones and Bloom, 1981). The net consequence of these changes for XII MN excitability is apparent in the well-established decrease in airway tone that occurs during sleep (Sauerland and Harper, 1976; Remmers et al., 1978) and contributes to OSA. Extensive resources have been devoted to identifying mechanisms underlying the muscle atonia of REM sleep. The rational is that once identified, receptor, second messenger or effector diversity will enable the change underlying reduced airway tone to be selectively reversed pharmacologically and obstructive apneas reduced with minimal side-effects.

The two main mechanisms proposed to underlie this state-dependent fall in MN output are active inhibition and aminergic disfacilitation (withdrawal of excitatory modulatory input) (Kubin et al., 1998). A series of heroic studies in the 1980s using intracellular recording and juxtacellular drug application methods to record activity of spinal and trigeminal MNs in naturally sleeping cats led to the largely unchallenged view (until recently Brooks and Peever, 2008) that in most MNs active inhibition is primarily responsible for the atonia of REM sleep (Morales and Chase, 1978, 1981, 1982; Morales et al., 1987; Soja et al., 1987; Chase et al., 1989). In contrast, a large body of elegant work over the last three decades in the carbachol model of REM sleep (Kubin et al., 1993, 1994; Fenik et al., 2004, 2005b,c, 2008) and more recently in unrestrained animals chronically instrumented with electromyographic (EMG) electrodes to monitor MN activity and microdialysis probes for infusion of drugs into the XII nucleus (Morrison et al., 2003; Sood et al., 2005; Chan et al., 2006; Sood et al., 2007), underlies the general opinion that atonia in XII MNs results primarily from disfacilitation (Kubin et al., 1998; Horner, 2008a, 2009); i.e., different mechanisms are proposed to underlie atonia in the spinal and trigeminal compared to XII MNs.

Despite this intense scrutiny of XII MN properties and mechanisms underlying XII atonia, little progress has been made in converting this information into a pharmacological therapy for OSA. Numerous clinical trials (summarized in Dempsey et al., 2010) designed to maintain aminergic tone during sleep (especially REM sleep), have produced unremarkable results. This consistent failure raises many questions including the extreme but unlikely possibility that mechanisms identified in rats and cats do not apply to humans. Another possibility is that multiple modulatory systems contribute to the production of REM atonia (Horner, 2008a, 2009) and that counteracting aminergic disfacilitation alone is insufficient to overcome the other factors. Consistent with this possibility are experiments describing active inhibition in XII MNs during carbachol-evoked and natural REM sleep (Yamuy et al., 1999; Engelhardt et al., 2004). Cholinergic mechanisms are also likely to contribute as nicotinic and muscarinic receptors have multiple excitatory and inhibitory actions on XII MNs, both in vitro and in anesthetized animals (Bellingham and Berger, 1996; Bellingham and Funk, 2000; Robinson et al., 2002; Liu et al., 2005). Which of these cholinergic mechanisms predominates during wakefulness and various sleep states, however, is not known.

The inefficacy of aminergic therapies to alleviate OSA may also reflect the diverse actions of aminergic signaling in the CNS. It may be optimistic to assume that systemic delivery of even the best cocktail of drugs will effectively treat OSA because multiple adverse effects may occur at doses lower than required to counteract the effects of aminergic disfacilitation on MN excitability in REM sleep. In addition, increasing evidence suggests that the disease process of OSA itself, in particular the chronic episodes of hypoxia/reoxygenation, not only causes oxidative injury to XII MNs, it also damages wake-active dopaminergic and noradrenergic neurons (Veasey et al., 2004; Zhan et al., 2005; Zhu et al., 2007; Lim and Veasey, 2010). This damage may compromise the capacity of XII MNs to respond to aminergic modulation. In addition, if noradrenergic neurons are sufficiently affected, the ability of NE uptake blockers to elevate extracellular monoamine levels may be reduced. Sleep loss alone, independent of hypoxia, may also limit MN plasticity and impair adaptive responses (Tadjalli and Peever, 2010b). Disease-dependent processes that potentially modify the normal control mechanisms and the clinical implications of these modifications have recently been reviewed (Dempsey et al., 2010).

The significance for REM atonia and OSA of noradrenergic receptor-mediated forms of ventilatory long-term facilitation (vLTF) that can be evoked by intermittent hypoxia, intermittent α_1 receptor stimulation, or disruptions in vagal mechanoreceptor feedback that will accompany apnea are also unknown (Neverova et al., 2007; MacFarlane et al., 2008; Mahamed and Mitchell, 2008; Tadjalli et al., 2010a). These forms of plasticity are proposed to be protective and preserve airway patency by acutely increasing motor output. vLTF does appear enhanced in non-REM (NREM) sleep, consistent with such a role. However, chronic intermittent hypoxia (which simulates OSA) induces metaplastic events that influence the capacity for vLTF (MacFarlane et al., 2008). In this context, the severity of the chronic intermittent hypoxia may be critical. Moderate CIH enhances vLTF (Wilkerson and Mitchell, 2009) while severe CIH appears to block vLTF (Veasey et al., 2004).

The focus of this section is on the basic mechanisms underlying REM sleep atonia in XII MNs in normal mammals. Specifically, our objective is to revisit the debate concerning the relative roles of aminergic disfacilitation vs. active inhibition in mediating the atonia of REM sleep at the XII nucleus. Data are presented from the perspective that the focus on active inhibition in spinal MNs, but disfacilitation in XII MNs reflects in part technical limitations associated with methods used to assess MN excitability. While the focus on mechanisms underlying the atonia of REM sleep makes the discussion most relevant to OSA that occurs in REM sleep, its relevance is not limited to REM sleep because the transition from wakefulness, to slow-wave-sleep to REM sleep is associated with progressive reductions in aminergic cell activity.

The muscle atonia of REM sleep is a signature feature of this state that distinguishes it from slow wave or NREM sleep and wakefulness. Its functional significance is not completely known but the violent and potentially harmful body movements of patients with REM behaviour disorder (Sforza et al., 2004) highlight the importance of paralyzing muscles during this phase of sleep, which, in terms of brain activity is much more like wakefulness than NREM sleep. Mechanistically, it is important to emphasize that OSA is specific to sleep. Even patients with the most severe cases breathe normally when awake. Thus, OSA is ultimately caused by the actions of the networks that control sleep on the motor networks that control motor outflow to the pharyngeal muscles, which during wakefulness is sufficient to keep the airway open (Mezzanotte et al., 1992).

The current debate about mechanisms underlying the atonia of REM sleep in the genioglossus and other airway muscles centers on whether it is mediated by glycinergic inhibition OR aminergic disfacilitation. We therefore review the evidence supporting these two views before presenting the rational for an emerging view that REM atonia results from a combination of these two mechanisms (Horner, 2009; Dempsey et al., 2010).

Mechanisms of REM sleep atonia: active inhibition VERSUS aminergic disfacilitation

The behavioural state of REM sleep, first defined more than 50 years ago (Aserinsky and Kleitman, 1953), is characterized in mammals by fast, desynchronized rhythms in the cortical EEG, rapid eye movements, autonomic activation and reduced muscle tone. Neither the neural circuit regulating

REM sleep, nor the mechanisms underlying these hallmark features of REM sleep are fully resolved, including those mediating muscle atonia. Candidate cell groups and transmitter systems underlying this atonia are those that show significant state-dependent changes in activity and modulate MN excitability, either directly or indirectly, and include glycine, GABA, norephineprhine, dopamine, serotonin, histamine, and acetylcholine (Horner, 2009; Dempsey et al., 2010). The pathways to be discussed here are postsynaptic glycinergic/GABAergic inhibition and NE/serotonin (5HT) disfacilitation.

Active inhibition. That lumbar and trigeminal MNs receive REM-sleep specific glycinergic inhibition was established in the 80's by a series of intracellular recording studies, which incorporated 5 barrel drug pipettes for juxtacellular application of transmitter antagonists to demonstrate MN hyperpolarization and their bombardment by strychnine-sensitive inhibitory postsynaptic potentials (IPSPs) during REM sleep (Chase et al., 1989; Soja et al., 1991; Yamuy et al., 1999). All measureable REM-specific changes in membrane properties were blocked by strychnine. Similarly, convincing data were generated for trigeminal MNs. Minor contributions from other transmitters were not excluded. A minor role for aminergic disfacilitation was considered possible since levels of 5HT and norepinephrine in spinal cord and XII microdialysates decrease in carbachol-evoked REM (Kubin et al., 1994; Lai et al., 2001). Nevertheless, the resolution afforded by directly measuring membrane potential, and the discrete application of drugs to the recorded MN provided compelling evidence that active inhibition is the main mechanism of atonia in lumbar and trigeminal MNs. Challenges to this view have been rare. However, trigeminal EMG data from a model that has focused attention on aminergic disfacilitation in atonia in XII MNs have been cited in support of the hypothesis that aminergic disfacilitation also dominates in trigeminal MNs (Brooks and Peever, 2008).

Aminergic disfacilitation. Noradrenergic inputs to the XII nucleus derive from pontine A5 and A7 cell groups and the LsC (Aldes et al., 1992), while those to spinal MNs derive from A5, A7 and locus coeruleus (LC) (Fritschy and Grzanna, 1990). 5HT innervation of XII and spinal MNs comes from the dorsal and medullary raphe nuclei (Jacobs and Fornal, 1991; Jacobs and Azmitia, 1992). Noradrenergic LC and LsC neurons (Aston-Jones and Bloom, 1981; Reiner, 1986), like 5HT raphe neurons, are classic REM-OFF neurons. They are highly active during wakefulness, less active during NREM sleep and silent during REM sleep. State-dependent activity patterns of A5 and A7 groups are unknown, but c-fos studies suggest they are also inactive during REM sleep (Rukhadze et al., 2007a). The primary action of NE on MNs, including XII MNs, is an α_1 receptor-mediated, postsynaptic excitation (Parkis et al., 1995; Volgin et al., 2001) (see Section *Ontogeny of noradrenergic receptor subtype expression in XII motoneurons*). The postsynaptic effects of 5HT on MN excitability change developmentally, but in juvenile rats are similar to those of NE and, in fact, they may actually converge on many of the same signaling cascades and effectors (Rekling et al., 2000). 5HT also acts presynaptically via $5HT_{1B}$ receptors to inhibit transmitter release (Singer et al., 1996).

These observations that the actions of monoamines on MNs are primarily excitatory, and the activity of monoaminergic neurons essentially stops in REM, underlie the long-standing hypothesis that levels of NE and 5HT in motor nuclei decrease with transitions to REM sleep and MN activity will fall due to disfacilitation (Kubin et al., 1998). In trigeminal and spinal MNs, evidence supporting a role for aminergic disfacilitation in REM atonia is equivocal, and primarily limited to microdialysis studies showing that the release of 5HT and NE in lumbar ventral horn is reduced during REM sleep-like atonia in cats (Lai et al., 2001). In marked contrast, the majority of data relevant to airway MNs suggest that active inhibition does not play a significant role in REM-sleep atonia (Kubin et al., 1993; Morrison et al., 2003; Fenik et al., 2004; Fenik et al., 2005b,a; Sood et al., 2005; Chan et al., 2006; Horner, 2009), and that the primary mechanism is aminergic disfacilitation. These data derive primarily from extensive studies by Leszek Kubin and colleagues using XII nerve recordings in the carbachol model of REM sleep atonia, and Richard Horner using EMG recording in a preparation that allows drug delivery to motor nuclei via microdialysis in unrestrained rats. Administration of glycinergic antagonists to the XII nucleus in these two model systems during wake and NREM sleep does not prevent the loss of EMG activity that occurs with transitions into REM sleep. In contrast, microdialysis of 5HT antagonists and

especially norepinephrine antagonists into XII prior to REM sleep blocks XII EMG activity and prevents further reductions in EMG tone with transition to REM. Challenges to the primacy of disfacilitation in XII atonia have also been rare (Kubin et al., 1998; Morrison et al., 2003; Fenik et al., 2004; Fenik et al., 2005b,a; Sood et al., 2005; Chan et al., 2006; reviewed in Kubin et al., 1998; Horner, 2008b, a, 2009). However, as pointed out recently by Horner (2009), intracellular recording data in the carbachol model (Yamuy et al., 1999) and natural REM sleep showing glycinergic IPSPs at REM onset (Engelhardt et al., 2004), suggest that active inhibition contributes to REM atonia in XII MNs.

Mechanisms of REM sleep atonia: active inhibition AND aminergic disfacilitation

Where does this leave us with respect to the relative role of active inhibition *vs*. disfacilitation in REM sleep atonia? The earlier theme that different mechanisms underlie REM atonia in XII MNs (disfacilitation) compared to spinal and trigeminal MNs (active inhibition) is less compelling given evidence that inhibition AND disfacilitation both contribute in XII and spinal/trigeminal MNs. In reviewing the literature, one pattern consistently emerges, regardless of whether data were derived in spinal, trigeminal or XII nuclei, in the carbachol model in cat or rat, or in natural REM (cat and rat), using iontophoresis, pressure injection or microdialysis. When intracellular recording methods are used to assess MN activity and examine mechanisms of REM atonia, active inhibition is detected; when EMG activity is used as an index of MN activity, disfacilitation is most readily detected.

One implication of this correlation is that EMG recording of muscle activity during microdialysis of agents into motor nuclei is predisposed to detect disfacilitation whereas intracellular recording from individual MNs across states during juxtacellular iontophoresis of drugs is predisposed to detect active inhibition. Indeed, EMG recording is limited in its ability to detect active inhibition. This reflects in part that the EMG signal can only provide information on MN excitability in the range where membrane potential is above threshold and the MN is firing action potentials. Once the membrane potentials of the MNs innervating the recorded muscle fibers fall below threshold, the EMG falls silent and it will not detect further reductions in excitability associated with active inhibition. The ability of EMG recording to detect active inhibition in studies of REM sleep is further confounded because the physiology constrains the protocols that can use EMG to assess the role of active inhibition, and they both rely on negative responses. The first standard protocol is to apply glycine/GABA antagonists prior to REM onset and then assess if the atonia produced in the subsequent REM transition differs from control REM (no antagonists). REM atonia still occurs under these conditions (Kubin et al., 1993; Morrison et al., 2003; Brooks and Peever, 2008). One interpretation is that REM atonia is caused by mechanisms other than glycine- or GABA-mediated inhibition (e.g., disfacilitation). While potentially correct, there is a potential problem with this rationale. The addition of glycine antagonists in wake or NREM sleep will remove ongoing inhibition. Depending on baseline glycinergic activity, this has no effect or increases NREM EMG activity (Morrison et al., 2003; Brooks and Peever, 2008). Reductions in EMG activity with the next NREM-REM transition will correctly provide evidence that inhibition mediated by glycine is not the sole cause of REM atonia. The limitation, however, is that analysis of spinal MNs suggests that aminergic disfacilitation alone is sufficient to essentially silence MNs (Heckmann et al., 2005; Heckman et al., 2008). If only recording EMG under these conditions, the REM atonia would appear fully developed regardless of whether there was a contribution of glycinergic inhibition. If disfacilitation is similarly effective at silencing XII MNs, then EMG recording alone will be insufficient to detect a role for active inhibition.

The second protocol that measures motor nerve of EMG activity to assess the role of active inhibition in REM is to block aminergic activity prior to REM onset (Fenik et al., 2005b, a; Chan et al., 2006). This reduces MN and EMG activity. No additional reduction in activity with the next transition to REM sleep may then be correctly interpreted as evidence that active inhibition does not contribute to REM atonia. As above, however, the problem of interpretation comes when blocking aminergic activation prior to REM completely silences MNs because it is no longer possible to detect an additional decrease in nerve or EMG activity; i.e., a REM-specific glycinergic inhibition could easily go undetected with this

method. Protocol variations that have been used to address this limitation include addition of CO_2 to the inspired gas, which increases inspiratory drive and MN activity. Excitatory agents are also added to increase baseline EMG activity prior to REM so that an inhibition can be detected via MN or EMG recording (Fenik et al., 2004, 2005a,b; Brooks and Peever, 2008). While these introduce the potential for drug interactions, and are confounded by the difficulty of activating EMG once it is suppressed in REM, they are useful and in general reveal an inhibitory component to REM atonia (Horner, 2009; Brooks and Peever, 2010).

Conversely, while intracellular recording experiments that used juxtacellular iontophoresis of strychnine were ideally designed to detect active postsynaptic inhibition of MNs during REM sleep (Morales and Chase, 1978, 1981, 1982; Chase and Morales, 1983; Morales et al., 1987; Soja et al., 1987), they are less likely to detect aminergic disfacilitation. This reflects that intracellular recording most directly samples the soma and proximal dendrites where glycinergic inputs are more concentrated. Aminergic inputs are more diffusely distributed (Rekling et al., 2000). If both inputs are active simultaneously, the proximal inhibitory inputs could shunt aminergic actions. Similarly, activation of glycinergic inputs in REM could make it difficult to detect changes in membrane properties associated with the simultaneous removal of aminergic inputs. Moreover, if PICs are dendritic, as appears to be the case for spinal and XII MNs, specific protocols are required to detect their effects on MN excitability. These protocols have not been applied to XII MNs (or any MN) during natural sleep-wake cycling. A developmental analysis of the multicomponent XII MN PIC and its amine sensitivity is required, along with in vivo assessments of its magnitude across sleep-wake states.

A model of REM atonia involving inhibition and disfacilitation also offers plausible mechanistic explanations for consistent but poorly understood observations. High on this list is the apparent insensitivity of muscle to excitatory input once its output is suppressed in REM sleep. Applications of NE, 5HT and glutamate that evoke powerful EMG responses in wakefulness, NREM sleep and even anesthesia are without effect in natural REM sleep (Chan et al., 2006; Brooks and Peever, 2008; Horner, 2008b). This parallels the clinical observation that when the airway is obstructed in sleep, airway muscle is very difficult to reactivate (Horner, 1996). One hypothesis is that the signaling pathways for these agents are blocked (Chan et al., 2006). However, a dual mechanism of inhibition and disfacilitation could explain most experimental observations. For example, that strychnine alone does not restore MN excitability in REM could reflect extremely low sensitivity of dendrites to synaptic inputs in the absence of monoamines. The insensitivity of trigeminal EMG to glutamatergic inputs in REM (Brooks and Peever, 2008) could similarly reflect low monoamine levels, small PIC amplitude and minimal amplification. Spinal MN responses to glutamatergic, synaptic inputs from Ia afferents fall dramatically when PICs are reduced via aminergic antagonists, or acute spinal cord transection (Bennett et al., 2001; Heckman et al., 2008). Similarly, our preliminary data in XII MNs reveal that inhibition of the PIC, I_{CAN}, by flufenamic acid (100 μM) blocks the ability of α_1 noradrenergic receptors to amplify glutamate inputs (Fig. 5). Conversely, the observation in REM sleep that NE alone does not restore XII MN excitability to control levels (Chan et al., 2006) may reflect that active inhibition can shunt and negate the effects of monoamines on more distal dendrites. Note, however, there is no direct evidence that XII MN sensitivity to synaptic inputs is reduced in REM. The best evidence is that the EMG is insensitive to excitatory input in REM. Intracellular recordings from XII MNs during natural REM sleep will be required to determine whether lack of EMG responses to excitatory inputs in REM sleep reflects that: i) MNs are sensitive but remain below threshold due to inhibition; ii) MN sensitivity to excitatory inputs is lost due to reduction in PICs, or; iii) MN sensitivity to amines is blocked (Chan et al., 2006).

Functional compartmentalization of the dendritic tree

Full understanding of the significance of any modulator for information processing requires that the spatial distribution of the modulatory input on the somatodendritic tree and its pattern of activation be determined in relation to the distribution of the different functional classes of input. Such segregation of afferent fields has profound implications for understanding synaptic integration. For MNs which

participate in multiple behaviors (Dickinson, 1995; Gestreau et al., 2005), spatial segregation of different functional inputs would provide a convenient means of "gating" the different drives since dendritic inhibition can control the weight of excitatory inputs from different dendritic regions (Skydsgaard and Hounsgaard, 1994). It would also provide a convenient means for modulators to influence specific functional classes of input. Despite the importance of the spatial distribution of synaptic and modulatory inputs, it remains uncertain whether synapses underlying a specific functional input, or modulatory input, are evenly distributed over the entire dendritic tree or spatially segregated to discrete regions. The diffuse nature of NE inputs to most motor nuclei and the likelihood, based on inability to detect close appositions between NE-containing varicosities and XII MNs innervating the genioglossus (Gatti et al., 2002), suggests that its effects are mediated through volume transmission. Volume transmission, as Golgi described it a century ago, is a means of "setting entire provinces of the CNS … to an appropriate functional state so they work as a unit" (see Agnati et al., 1995). The expectation therefore is that NE will have a uniform effect on all dendritic compartments and that the consequences of NE modulation are similar for all classes of input.

This view, however, is challenged by our observation that, while NE and Substance-P inputs converge on a common transduction pathway (Talley et al., 2000), and have virtually identical effects on membrane properties and repetitive firing responses to somally injected current, NE is ~3-fold more effective in potentiating endogenous inspiratory inputs (Yasuda et al., 2001). The greater efficacy of NE may simply reflect potentiation of glutamatergic inspiratory currents. However, it may also reflect functional compartmentalization of the dendritic tree such that compared to SP, NE inputs and/or α_{1B} receptors may be preferentially distributed on dendrites that receive inspiratory inputs. A further implication is that SP may be important in non-respiratory functions of XII MNs. It has been suggested that XII MN dendrites extending ventrolaterally may be the target of inspiratory preMNs while those extending ventrally receive inputs from Raphe neurons (Nunez-Abades et al., 1994). However, it remains unclear in XII MNs whether synapses underlying a specific functional input, or modulatory input, are evenly distributed over the entire dendritic tree or spatially segregated to discrete dendritic compartments.

To directly test the hypothesis that NE inputs are preferentially distributed to regions receiving inspiratory inputs will require a combination of functional imaging and immunohistochemical techniques to visualize the distribution of active glutamatergic inspiratory synapses on the XII MN dendritic tree in relation to active NE terminals and postsynaptic α_1 receptors. At present, however, technologies for imaging dendrites with the spatial and temporal resolution necessary to map active synapses are limited to small portions of the dendritic tree. As an initial step, we have combined electrophysiology, immunohistochemistry and confocal microscopy to determine whether NE-immunolabeled terminals are distributed randomly relative to the dendritic tree of biocytin-labeled inspiratory XII MNs or preferentially distributed around specific parts of the tree.

Confocal images acquired using sequential excitation at 488 (to image MN morphology) and 568 nm (to image NE terminals) were analysed using Interactive Data Language 5.5 to assess the radial distribution of NE immunlabeled varicosities within 10 μm of XII MN dendrites. High density of NE labeled varicosities in close proximity (< 1 μm) to a dendritic process and progressively lower density at increasing radial distances would be consistent with a preferential distribution of NE near the dendrites. Flat, uniform distribution plots would suggest a random distribution of NE.

We examined 48 dendrite segments from 9 XII MNs with a mean (± SEM) whole-cell capacitance of 27 ± 2 pF, resting membrane potential of -54 ± 1 mV and input resistance of 181 ± 8 MΩ. All cells lay within 200 μm of obex in the ventromedial portion of the XII nucleus (Fig. 7). An extensive plexus of NE-immunoreactive fibres extended throughout the XII nucleus, punctuated along their extent by numerous varicosities (Fig. 7C, D). To quantitatively assess whether NE immunoreactivity is distributed randomly throughout the XII nucleus or preferentially distributed in close proximity to the somatodendritic tree of XII MNs, we analyzed the radial distribution of NE immunofluorescence around individual MN dendrites by calculating how the proportion of volume around the dendrite occupied by NE varicosities changed as the volume was expanded radially.

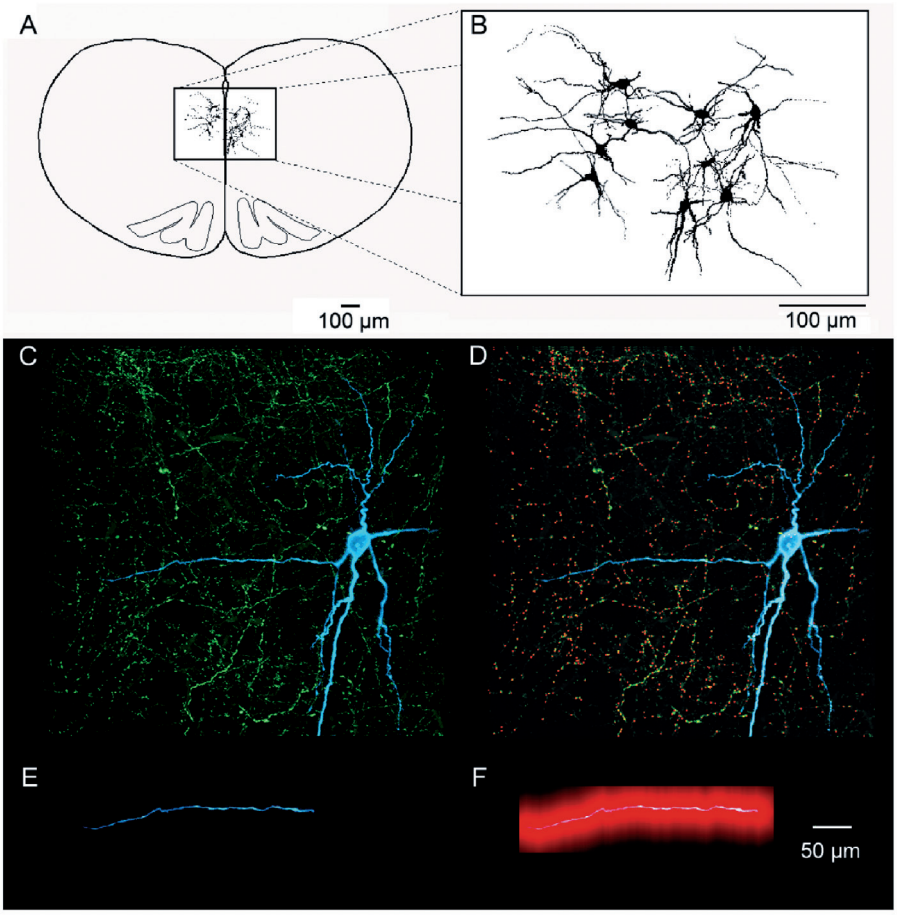

Fig. 7. - XII motoneurons are surrounded by a dense plexus of NE immunolabeled fibers. A) Schematic showing location of labelled XII MNs and their dendritic fields in the transverse plane of the mouse medulla. B) Composite projection of nine XII MNs filled with Biocytin using the whole-cell patch technique and visualized by confocal fluorescence of Extravidin conjugated Alexa™488. C) Maximum projection of an Alexa™488 labelled XII MN (blue) and norepinephrine labelled with rabbit anti-NE primary antibody and an Alexa™568 conjugated anti-rabbit secondary antibody (green). Large NE varicosities and connecting thread like structures are visible. D) Overlay of identified varicosities (red) on NE immunofluorescence signal (green). E) Single dendrite of XII MN reconstructed in 3-dimensions. F) Distance map of the space around the dendrite defining the distance from every voxel in the sub-volume to the nearest point of the dendrite. Methods: After 30-60 min of whole-cell recording (pipettes contained 0.2-0.5% Biocytin to label the MNs for morphological reconstruction), the 200 µm thick sections containing biocytin-filled MNs were fixed (5% glutaraldehyde), and incubated with Extravidin conjugated Alexa™488 in phosphate buffered saline (PBS with 0.4% Triton X-100 (PBS-Triton) for 24 hours. For NE immunohistochemistry, sections were pre-incubated with 10% sheep serum in PBS-Triton (1 h, room temperature), incubated in PBS-Triton containing 5% sheep serum, 0.01% sodium azide and rabbit IgG antibody to NE (1:500; Chemicon, 72 h, 4°C). Sections were washed (3 x 30 min, PBS-Triton), incubated (24 h, 4°C) with Alexa™568-conjugated goat anti-rabbit IgG (1:500, Molecular Probes), washed (3 x 30 min, PBS-Triton) and mounted in Citifluor™. Sections were imaged using a Leica™ TCS-SP2 (Leica Microsystems) laser-scanning confocal microscope with an argon/krypton mixed gas laser. The 488 and 543 laser lines were used to excite Alexa™488 and Alexa™568 respectively. Optical sections were collected at 0.3 to 0.7 µm resolution using a Leica x40 oil-immersion objective. Sequential four-frame averages were collected using emission bands of 475-550 nM to image Alexa™488 labeling and 550-650 nM to image Alexa™568 labelling. MN morphology and the distribution of NE immunolabelling were reconstructed from serial optical sections using Interactive Data Language (IDL) version 5.5 (Research Systems Inc). Distribution of the NE immunofluorescence relative to the MN dendrites was assessed by analyzing the density of NE labelling in regions surrounding dendritic segments. Dendritic segments that remained in a relatively uniform z-plane were selected for analysis to eliminate potential problems associated with non-uniform antibody penetration in the z-axis as well as non-uniform laser penetration. Sub-volumes were created that contained each dendritic segment and surrounding local space up to a distance of 10 µm (E). An identical sub-volume was created for the NE immunoreactive field. A 3-dimensional mask of the dendrite was created within the NE field and a distance map of the space around the dendrite created (F). This distance map defined the distance from every voxel (3-D equivalent of a pixel) in the sub-volume to the nearest point of the dendrite and was used to determine, as a function of distance from the dendrite, the fraction of the volume surrounding the dendrite occupied by NE immunofluorescence.

Tests of this technique using computer-generated, random and clustered NE distributions confirmed that a randomly distributed field of NE-containing fibers would produce a flat distribution plot while a field distributed preferentially in close proximity to the MN dendrites would produce a plot that peaked near the origin (the dendrite) and then declined with increasing distance from the origin (data not shown). Using this analysis the radial distribution of NE immunoreactivity around individual dendrites on the same cell was found to be highly variable. Some dendrites had levels of NE that declined with increasing radial distance (Fig. 8A, dendrites a, c & d), while others had low NE labelling close to the dendrite (Fig. 8B, dendrite b). Of 48 dendrite segments analyzed, 15 exhibited a distribution profile that peaked within the first 1 μm and declined with increasing radial distance. To assess the likelihood that these distributions

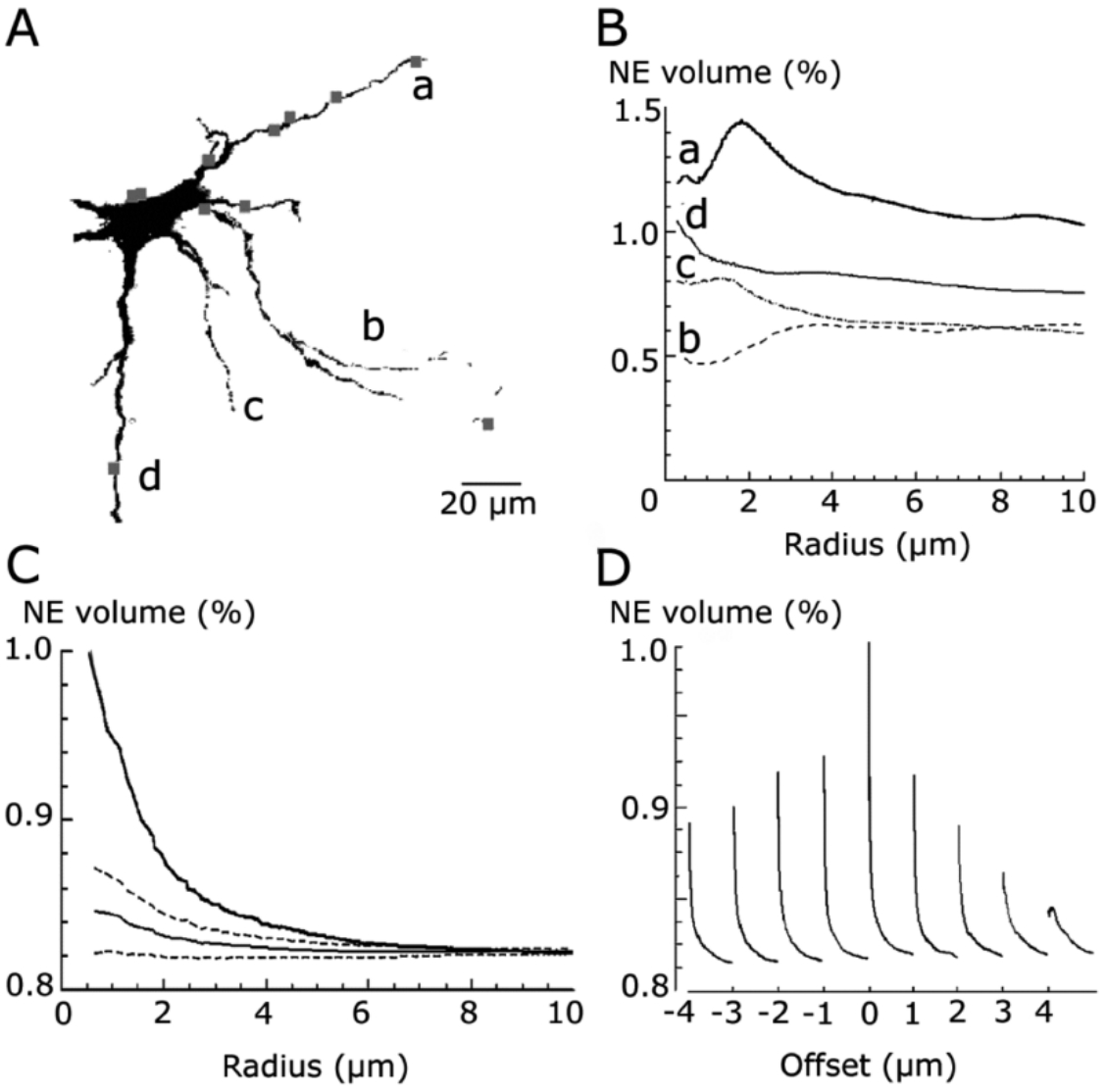

Fig. 8. - Noradrenergic modulation of XII motoneuron dendritic tree may not be uniform but compartmentalized. A) Location of 11 NE varicosities (grey) found within 1.5 μm of the cell soma and dendrites. B) Plots of NE density as a function of distance from the cell and some of its processes (a,b,c,d) reveal a non-uniform distribution of norepinephrine, with concentrations falling as distance from the cell increases for some of the dendrites (a, d, c) but not others (b). C) Distribution of NE immunofluorescence around dendrite "d" and the mean ±95% CI for random alignment of the NE field. D) Distribution of data for dendrite "d" misaligned by ±1-4 μm in the x-plane indicating that highest NE immunofluorescence is detected at the origin.

were obtained by chance, multiple distribution plots for each dendrite segment were calculated using 20 randomly misaligned NE datasets in order to generate mean distribution ±95% CI plots against which correctly aligned data were compared. Eleven of these 15 dendritic segments exhibited a distribution plot in which the peak over the first 1 μm exceeded the 95% CI for random alignment (Fig. 8C). Thus, every MN examined had at least one dendritic segment that received noradrenergic innervation at a concentration higher than would be expected by chance alone. Further confirmation was sought by misaligning the data fields by ±0.3-3 μm in the x-plane to test that the highest peak was generated at the origin. In 8 of these 11 dendrite segments, the highest distribution peak was generated at the origin (Fig. 8D).

While our analysis was limited to primary and secondary dendrites, data suggest that the dendritic tree does not receive a uniform noradrenergic innervation but is compartmentalized. Functionally, the implication is that noradrenergic inputs will differentially modulate inputs arriving on different parts of the dendritic tree. Whether the regions of the tree receiving the greatest NE innervation receive a prominent inspiratory input, and whether this distribution changes developmentally remain to be determined. In addition, if NE is released via volume transmission it remains possible that a uniform concentration of NE will be established within the XII nucleus, despite a non-uniform distribution of varicosities, especially at high levels of NE cell activity. The heterogeneous distribution of varicosities however, supports compartmentalized modulation of the dendritic tree, at least during periods when NE neuron activity is low.

Summary

In summary, we have presented evidence that maturation of the noradrenergic network that modulates XII MN excitability is a highly coordinated process involving parallel development of MN sensitivity, noradrenergic neurons that project to the XII nucleus and the innervation of the XII nucleus by NE nerve terminals. One consequence of this developmental process is an augmented potentiation of XII inspiratory output, which may serve to maintain airway stability in the face of developmental reductions in intrinsic MN excitability. Given the demonstrated potential for compartmentalized modulation of the dendritic tree, determining whether this enhancement of excitability applies to all classes of synaptic input or is specific for inspiratory drive will require examination of functionally-identified inputs that are processed by the dendritic tree in a physiological manner.

On faster time scales, while active inhibitory mechanisms (as well as cholinergic and other monoaminergic systems) should not be overlooked, noradrenergic disfacilitation is a major factor in the state-dependent control of XII MN excitability. Cellular mechanisms underlying NE disfacilitation will include loss of TASK1/TASK3 K^+ channel inhibition and the associated hyperpolarization and decreased R_N. However, based on the presence of PICS in XII MNs and the importance of amine-sensitive PICS in maintaining the excitability of spinal MNs, downregulation of amine-sensitive PICs in REM sleep is a potentially significant contributor to REM sleep atonia that demands further examination not only in XII MNs but MNs in general.

Acknowledgements

This work was supported by the Alberta Heritage Foundation for Medical Research (AHFMR), Canadian Institute for Health Research (CIHR), Canadian Foundation for Innovation (CFI), and the Alberta Science and Research Authority (ASRA), Women and Children's Health Research Institute, Auckland Medical Research Foundation, Health Research Council of New Zealand and the Marsden Fund. GDF is an AHFMR Scientist.

References

Adachi T., Robinson D.M., Miles G.B., Funk G.D. Noradrenergic modulation of XII motoneuron inspiratory activity does not involve alpha$_2$-receptor inhibition of the I_h current or presynaptic glutamate release. *J. Appl. Physiol.*, **98**: 1297-1308, 2005.

Adachi T., Huxtable A.G., Fang X., Funk G.D. Substance P modulation of hypoglossal motoneuron excitability during development: changing balance between conductances. *J. Neurophysiol.*, **104**: 854-872, 2010.

Agnati L.F., Zoli M., Strömberg I., Fuxe K. Intercellular communication in the brain: wiring versus volume transmission. *Neuroscience*, **69**: 711-726, 1995.

Aldes L.D. Topographically organized projections from the nucleus subceruleus to the hypoglossal nucleus in the rat: a light and electron microscopic study with complementary axonal transport techniques. *J. Comp. Neurol.*, **302**: 643-656, 1990.

Aldes L.D., Chapman M.E., Chronister R.B., Haycock J.W. Sources of noradrenergic afferents to the hypoglossal nucleus in the rat. *Brain Res. Bull.*, **29**: 931-942, 1992.

Aldes L.D., Bartley K., Royal K., Dixon A., Chronister R.B. Pre- and postnatal development of the catecholamine innervation of the hypoglossal nucleus in the rat: an immunocytochemical study. *Brain Res. Dev. Brain Res.*, **91**: 83-92, 1996.

Alonso-Llamazares A., Zamanillo D., Casanova E., Ovalle S., Calvo P., Chinchetru M.A. Molecular cloning of alpha 1d-adrenergic receptor and tissue distribution of three alpha 1-adrenergic receptor subtypes in mouse. *J. Neurochem.*, **65**: 2387-2392, 1995.

Aserinsky E. and Kleitman N. Regularly occurring periods of eye motility, and concomitant phenomena, during sleep. *Science*, **118**: 273-274, 1953.

Aston-Jones G. and Bloom F.E. Activity of norepinephrine-containing locus coeruleus neurons in behaving rats anticipates fluctuations in the sleep-waking cycle. *J. Neurosci.*, **1**: 876-886, 1981.

Barnes K.L., Chernicky C.L., Block C.H., Ferrario C.M. Distribution of catecholaminergic neuronal systems in the canine medulla oblongata and pons. *J. Comp. Neurol.*, **274**: 127-141, 1988.

Bartlett D.J., Leiter J.C., Knuth S.L. Control and actions of the genioglossus muscle. In: Suratt F.G. and Remmers J.E. (Eds.) *Sleep and Respiration*, New York, Wiley-Liss: 99-108, 1990.

Bartolome J.V., Kavlock R.J., Cowdery T., Orband-Miller L., Slotkin T.A. Development of adrenergic receptor binding sites in brain regions of the neonatal rat: effects of prenatal or postnatal exposure to methylmercury. *Neurotoxicology*, **8**: 1-13, 1987.

Bayliss D.A., Viana F., Bellingham M.C., Berger A.J. Characteristics and postnatal development of a hyperpolarization-activated inward current in rat hypoglossal motoneurons in vitro. *J. Neurophysiol.*, **71**: 119-128, 1994.

Bayliss D.A., Viana F., Talley E.M., Berger A.J. Neuromodulation of hypoglossal motoneurons: cellular and developmental mechanisms. *Respir. Physiol.*, **110**: 139-150, 1997.

Bellingham M.C. and Berger A.J. Presynaptic depression of excitatory synaptic inputs to rat hypoglossal motoneurons by muscarinic M2 receptors. *J. Neurophysiol.*, **76**: 3758-3770, 1996.

Bellingham M.C. and Funk G.D. Cholinergic modulation of respiratory brain-stem neurons and its function in sleep-wake state determination. *Clin. Exp. Pharmacol. Physiol.*, **27**: 132-137, 2000.

Bennett D.J., Li Y., Siu M. Plateau potentials in sacrocaudal motoneurons of chronic spinal rats, recorded in vitro. *J. Neurophysiol.*, **86**: 1955-1971, 2001.

Berg A.P., Talley E.M., Manger J.P., Bayliss D.A. Motoneurons express heteromeric TWIK-related acid-sensitive K+ (TASK) channels containing TASK-1 (KCNK3) and TASK-3 (KCNK9) subunits. *J. Neurosci.*, **24**: 6693-6702, 2004.

Berger A.J., Bayliss D.A., Bellingham M.C., Umemiya M., Viana F. Postnatal development of hypoglossal motoneuron intrinsic properties. *Adv. Exp. Med. Biol.*, **381**: 63-71, 1995.

Berger A.J., Bayliss D.A., Viana F. Development of hypoglossal motoneurons. *J. Appl. Physiol.*, **81**: 1039-1048, 1996.

Berger A.J. Determinants of respiratory motoneuron output. *Respir. Physiol.*, **122**: 259-269, 2000.

Bieger D. Neuropharmacologic correlates of deglutition: lessons from fictive swallowing. *Dysphagia*, **6**: 147-164, 1991.

Brooks P.L. and Peever J.H. Glycinergic and $GABA_A$-mediated inhibition of somatic motoneurons does not mediate rapid eye movement sleep motor atonia. *J. Neurosci.*, **28**: 3535-3545, 2008.

Brooks P.L. and Peever J.H. GABAergic and glycinergic control of upper airway motoneurons in rapid eye movement sleep. *Adv. Exp. Med. Biol.*, **669**: 259-262, 2010.

Cameron W.E., Nunez-Abades P.A., Kerman I.A., Hodgson T.M. Role of potassium conductances in determining input resistance of developing brain stem motoneurons. *J. Neurophysiol.*, **84**: 2330-2339, 2000.

Chan E., Steenland H.W., Liu H., Horner R.L. Endogenous excitatory drive modulating respiratory muscle activity across sleep-wake states. *Am. J. Respir. Crit. Care Med.*, **174**: 1264-1273, 2006.

Chase M.H. and Morales F.R. Subthreshold excitatory activity and motoneuron discharge during REM periods of active sleep. *Science*, **221**: 1195-1198, 1983.

Chase M.H., Soja P.J., Morales F.R. Evidence that glycine mediates the postsynaptic potentials that

inhibit lumbar motoneurons during the atonia of active sleep. *J. Neurosci.*, **9**: 743-751, 1989.

Chen X., Talley E.M., Patel N., Gomis A., McIntire W.E., Dong B., Viana F., Garrison J.C., Bayliss D.A. Inhibition of a background potassium channel by Gq protein alpha-subunits. *PNAS*, **103** (9): 3422-3427, 2006.

Comings D.E., Gade-Andavolu R., Gonzalez N., Wu S., Muhleman D., Blake H., Dietz G., Saucier G., MacMurray J.P. Comparison of the role of dopamine, serotonin, and noradrenaline genes in ADHD, ODD and conduct disorder: multivariate regression analysis of 20 genes. *Clin. Genet.*, **57**: 178-196, 2000.

Dahlström A. and Fuxe K. Localization of monoamines in the lower brain stem. *Experientia*, **20**: 398-399, 1964.

Day H.E., Campeau S., Watson S.J.J., Akil H. Distribution of α_{1a}, α_{1b} and α_{1d}-adrenergic receptor mRNA in the rat brain and spinal cord. *J. Chem. Neuroanat.*, **13**: 115-139, 1997.

Dempsey J.A., Veasey S.C., Morgan B.J., O'Donnell C.P. Pathophysiology of sleep apnea. *Physiol. Rev.*, **90**: 47-112, 2010.

Denoroy L., Gay N., Gilly R., Tayot J., Pasquier B., Kopp N. Catecholamine synthesizing enzyme activity in brainstem areas from victims of sudden infant death syndrome. *Neuropediatrics*, **18**: 187-190, 1987.

Dickinson P.S. Interaction among neural networks for behavior. *Curr. Opin. Neurobiol.*, **5**: 792-798, 1995.

Dobbins E.G. and Feldman J.L. Differential innervation of protruder and retractor muscles of the tongue in rat. *J. Comp. Neurol.*, **357**: 376-394, 1995.

el Mansari M., Sakai K., Jouvet M. Unitary characteristics of presumptive cholinergic tegmental neurons during the sleep-waking cycle in freely moving cats. *Exp. Brain Res.*, **76**: 519-529, 1989.

Engelhardt J.K., Fung S.J., Yamuy J., Xi M.C., Morales F.R., Chase M.H. The unique inhibitory potentials in motoneurons that occur during active sleep are comprised of minimal unitary potentials. *Brain Res.*, **1018**: 26-31, 2004.

Falck B. and Torp A. New evidence for the localization of noradrenalin in the adrenergic nerve terminals. *Int. J. Exp. Med.*, **6**: 169-172, 1962.

Feldman J.L., Neverova N.V., Saywell S.A. Modulation of hypoglossal motoneuron excitability by intracellular signal transduction cascades. *Respir. Physiol. Neurobiol.*, **147**: 131-143, 2005.

Fenik V., Davies R.O., Kubin L. Combined antagonism of aminergic excitatory and amino acid inhibitory receptors in the XII nucleus abolishes REM sleep-like depression of hypoglossal motoneuronal activity. *Arch. Ital. Biol.*, **142**: 237-249, 2004.

Fenik V.B., Davies R.O., Kubin L. Noradrenergic, serotonergic and GABAergic antagonists injected together into the XII nucleus abolish the REM sleep-like depression of hypoglossal motoneuronal activity. *J. Sleep Res.*, **14**: 419-429, 2005a.

Fenik V.B., Davies R.O., Kubin L. REM sleep-like atonia of hypoglossal (XII) motoneurons is caused by loss of noradrenergic and serotonergic inputs. *Am. J. Respir. Crit. Care Med.*, **172**: 1322-1330, 2005b.

Fenik V.B., Ogawa H., Davies R.O., Kubin L. Carbachol injections into the ventral pontine reticular formation activate locus coeruleus cells in urethane-anesthetized rats. *Sleep*, **28**: 551-559, 2005c.

Fenik V.B., Rukhadze I., Kubin L. Inhibition of pontine noradrenergic A7 cells reduces hypoglossal nerve activity in rats. *Neuroscience*, **157**: 473-482, 2008.

Friedland D.R., Eden A.R., Laitman J.T. Naturally occurring motoneuron cell death in rat upper respiratory tract motor nuclei: a histological, fast DiI and immunocytochemical study in the hypoglossal nucleus. *J. Neurobiol.*, **27**: 520-534, 1995.

Fritschy J.M. and Grzanna R. Demonstration of two separate descending noradrenergic pathways to the rat spinal cord: evidence for an intragriseal trajectory of locus coeruleus axons in the superficial layers of the dorsal horn. *J. Comp. Neurol.*, **291**: 553-582, 1990.

Fukuda A., Nabekura J., Ito C., Plata-Salaman C.R., Oomura Y. Developmentally different onset of alpha 1- and alpha 2-adrenergic responses in the neonatal rat dorsal motor nucleus of the vagus in vitro. *Brain Res.*, **493**: 357-361, 1989.

Funk G.D., Smith J.C., Feldman J.L. Generation and transmission of respiratory oscillations in medullary slices: role of excitatory amino acids. *J. Neurophysiol.*, **70**: 1497-1515, 1993.

Funk G.D., Smith J.C., Feldman J.L. Development of thyrotropin-releasing hormone and norepinephrine potentiation of inspiratory-related hypoglossal motoneuron discharge in neonatal and juvenile mice in vitro. *J. Neurophysiol.*, **72**: 2538-2541, 1994.

Gatti P.J., Richardson K.A., Shirahata M., Johnson T.A., Coleman W., Massari V.J. *Soc. Neurosci. Abstr.*, **361**, 2002.

Gestreau C., Dutschmann M., Obled S., Bianchi A.L. Activation of XII motoneurons and premotor neurons during various oropharyngeal behaviors. *Respir. Physiol. Neurobiol.*, **147**: 159-176, 2005.

Happe H.K., Coulter C.L., Gerety M.E., Sanders J.D., O'Rourke M., Bylund D.B., Murrin L.C. Alpha-2 adrenergic receptor development in rat CNS: an autoradiographic study. *Neurosci.*, **123**: 167-178, 2004.

Heckmann C.J., Gorassini M.A., Bennett D.J. Persistent inward currents in motoneuron dendrites: implications for motor output. *Muscle Nerve*, **31**: 135-156, 2005.

Heckman C.J., Johnson M., Mottram C., Schuster J. Persistent inward currents in spinal motoneurons and their influence on human motoneuron firing patterns. *Neuroscientist*, **14**: 264-275, 2008.

Hilaire G. Endogenous noradrenaline affects the maturation and function of the respiratory network: Possible implication for SIDS. *Auton. Neurosci.*, **126-127**: 320-331, 2006.

Hokfelt T., Johansson O., Goldstein M. Chemical anatomy of the brain. *Science*, **225**: 1326-1334, 1984.

Horner R.L. Motor control of the pharyngeal musculature and implications for the pathogenesis of obstructive sleep apnea. *Sleep*, **19**: 827-853, 1996.

Horner R.L. Control of genioglossus muscle by sleep state-dependent neuromodulators. *Adv. Exp. Med. Biol.*, **605**: 262-267, 2008a.

Horner R.L. Neuromodulation of hypoglossal motoneurons during sleep. *Respir. Physiol. Neurobiol.*, **164**: 179-196, 2008b.

Horner R.L. Emerging principles and neural substrates underlying tonic sleep-state-dependent influences on respiratory motor activity. *Philos. Trans. R. Soc. Lond. B Biol. Sci.*, **364**: 2553-2564, 2009.

Jacobs B.L. and Fornal C.A. Activity of brain serotonergic neurons in the behaving animal. *Pharmacol. Rev.*, **43**: 563-578, 1991.

Jacobs B.L. and Azmitia E.C. Structure and function of the brain serotonin system. *Physiol. Rev.*, **72**: 165-229, 1992.

Jensen B.C., Swigart P.M., Simpson P.C. Ten commercial antibodies for alpha-1-adrenergic receptor subtypes are nonspecific. *Naunyn Schmiedebergs Arch. Pharmacol.*, **379**: 409-412, 2009.

Jones L.S., Gauger L.L., Davis J.N. Anatomy of brain alpha 1-adrenergic receptors: in vitro autoradiography with [125I]-heat. *J. Comp. Neurol.*, **231**: 190-208, 1985a.

Jones L.S., Gauger L.L., Davis J.N., Slotkin T.A., Bartolome J.V. Postnatal development of brain alpha 1-adrenergic receptors: in vitro autoradiography with [125I]HEAT in normal rats and rats treated with alpha-difluoromethylornithine, a specific, irreversible inhibitor of ornithine decarboxylase. *Neuroscience*, **15**: 1195-1202, 1985b.

Kalia M., Fuxe K., Goldstein M. Rat medulla oblongata. II. Dopaminergic, noradrenergic (A1 and A2) and adrenergic neurons, nerve fibers, and presumptive terminal processes. *J. Comp. Neurol.*, **233**: 308-332, 1985a.

Kalia M., Woodward D.J., Smith W.K., Fuxe K. Rat medulla oblongata. IV. Topographical distribution of catecholaminergic neurons with quantitative three-dimensional computer reconstruction. *J. Comp. Neurol.*, **233**: 350-364, 1985b.

Krammer E.B., Rath T., Lischka M.F. Somatotopic organization of the hypoglossal nucleus: a HRP study in the rat. *Brain Res.*, **170**: 533-537, 1979.

Kubin L., Kimura H., Tojima H., Davies R.O., Pack A.I. Suppression of hypoglossal motoneurons during the carbachol-induced atonia of REM sleep is not caused by fast synaptic inhibition. *Brain Res.*, **611**: 300-312, 1993.

Kubin L., Reignier C., Tojima H., Taguchi O., Pack A.I., Davies R.O. Changes in serotonin level in the hypoglossal nucleus region during carbachol-induced atonia. *Brain Res.*, **645**: 291-302, 1994.

Kubin L., Davies R.O., Pack A.I. Control of upper airway motoneurons during REM sleep. *News Physiol. Sci.*, **13**: 91-97, 1998.

Kubin L. and Volgin D.V. Developmental profiles of neurotransmitter receptors in respiratory motor nuclei. *Respir. Physiol. Neurobiol.*, **164**: 64-71, 2008.

Lai Y.Y., Kodama T., Siegel J.M. Changes in monoamine release in the ventral horn and hypoglossal nucleus linked to pontine inhibition of muscle tone: an in vivo microdialysis study. *J. Neurosci.*, **21**: 7384-7391, 2001.

Leung C.G. and Mason P. Physiological properties of raphe magnus neurons during sleep and waking. *J. Neurophysiol.*, **81**: 584-595, 1999.

Lim D.C. and Veasey S.C. Neural injury in sleep apnea. *Curr. Neurol. Neurosci. Rep.*, **10**: 47-52, 2010.

Liu X., Sood S., Liu H., Horner R.L. Opposing muscarinic and nicotinic modulation of hypoglossal motor output to genioglossus muscle in rats in vivo. *J. Physiol.*, **565**: 965-980, 2005.

Lorke D.E., Kwong W.H., Chan W.Y., Yew D.T. Development of catecholaminergic neurons in the human medulla oblongata. *Life Sci.*, **73**: 1315-1331, 2003.

MacFarlane P.M., Wilkerson J.E., Lovett-Barr M.R., Mitchell G.S. Reactive oxygen species and respiratory plasticity following intermittent hypoxia. *Respir. Physiol. Neurobiol.*, **164**: 263-271, 2008.

Mahamed S. and Mitchell G.S. Simulated apnoeas induce serotonin-dependent respiratory long-term facilitation in rats. *J. Physiol.*, **586**: 2171-2181, 2008.

Mansouri J., Panigrahy A., Assmann S.F., Kinney H.C. Distribution of alpha 2-adrenergic receptor binding in the developing human brain stem. *Pediatr. Dev. Pathol.*, **4**: 222-236, 2001.

McCune S.K., Voigt M.M., Hill J.M. Expression of multiple alpha adrenergic receptor subtype messenger RNAs in the adult rat brain. *Neuroscience*, **57**: 143-151, 1993.

Mezzanotte W.S., Tangel D.J., White D.P. Waking genioglossal electromyogram in sleep apnea patients versus normal controls (a neuromuscular compensatory mechanism). *J. Clin. Invest.*, **89**: 1571-1579, 1992.

Miles G.B., Lipski J., Lorier A.R., Laslo P., Funk G.D. Differential expression of voltage-activated calcium channels in III and XII motoneurones during development in the rat. *Eur. J. Neurosci.*, **20**: 903-913, 2004.

Miller J.F., Paul K.D., Lee R.H., Rymer W.Z., Heckman C.J. Restoration of extensor excitability in the acute spinal cat by the 5-HT_2 agonist DOI. *J. Neurophysiol.*, **75**: 620-628, 1996.

Mironov S.L. Metabotropic glutamate receptors activate dendritic calcium waves and TRPM channels which drive rhythmic respiratory patterns in mice. *J. Physiol.*, **586**: 2277-2291, 2008.

Morales F.R. and Chase M.H. Intracellular recording of lumbar motoneuron membrane potential during sleep and wakefulness. *Exp. Neurol.*, **62**: 821-827, 1978.

Morales F. and Chase M.H. Postsynaptic control of lumbar motoneuron excitability during active sleep in the chronic cat. *Brain Res.*, **225**: 279-295, 1981.

Morales F.R. and Chase M.H. Repetitive synaptic potentials responsible for inhibition of spinal cord motoneurons during active sleep. *Exp. Neurol.*, **78**: 471-476, 1982.

Morales F.R., Boxer P., Chase M.H. Behavioral state-specific inhibitory postsynaptic potentials impinge on cat lumbar motoneurons during active sleep. *Exp. Neurol.*, **98**: 418-435, 1987.

Moritz A.T., Newkirk G., Powers R.K., Binder M.D. Facilitation of somatic calcium channels can evoke prolonged tail currents in rat hypoglossal motoneurons. *J. Neurophysiol.*, **98**: 1042-1047, 2007.

Morrison J.L., Sood S., Liu H., Park E., Liu X., Nolan P., Horner R.L. Role of inhibitory amino acids in control of hypoglossal motor outflow to genioglossus muscle in naturally sleeping rats. *J. Physiol.*, **552**: 975-991, 2003.

Neverova N.V., Saywell S.A., Nashold L.J., Mitchell G.S., Feldman J.L. Episodic stimulation of alpha1-adrenoreceptors induces protein kinase C-dependent persistent changes in motoneuronal excitability. *J. Neurosci.*, **27**: 4435-4442, 2007.

Nicholas A.P., Pieribone V.A., Hokfelt T. Cellular localization of messenger RNA for beta-1 and beta-2 adrenergic receptors in rat brain: an in situ hybridization study. *Neuroscience*, **56**: 1023-1039, 1993.

Nicholas A.P., Hökfelt T., Pieribone V.A. The distribution and significance of CNS adrenoceptors examined with in situ hybridization. *Trends Pharmacol. Sci.*, **17**: 145-155, 1996.

Nilius B., Prenen J., Tang J., Wang C., Owsianik G., Janssens A., Voets T., Zhu M.X. Regulation of the Ca2+ sensitivity of the nonselective cation channel TRPM4. *J. Biol. Chem.*, **280**: 6423-6433, 2008.

Nunez-Abades P.A., Spielmann J.M., Barrionuevo G., Cameron W.E. In vitro electrophysiology of developing genioglossal motoneurons in the rat. *J. Neurophysiol.*, **70**: 1401-1411, 1993.

Nunez-Abades P.A., He F., Barrionuevo G., Cameron W.E. Morphology of developing rat genioglossal motoneurons studied in vitro: changes in length, branching pattern, and spatial distribution of dendrites. *J. Comp. Neurol.*, **339**: 401-420, 1994.

Nunez-Abades P.A. and Cameron W.E. Morphology of developing rat genioglossal motoneurons studied in vitro: relative changes in diameter and surface area of somata and dendrites. *J. Comp. Neurol.*, **353**: 129-142, 1995.

Nunez-Abades P.A. and Cameron W.E. Relationship between membrane properties and cell size of developing rat genioglossal motoneurons studied in vitro. *Neurosci. Lett.*, **223**: 41-44, 1997.

Pace R.W., Mackay D.D., Feldman J.L., Del Negro C.A. Inspiratory bursts in the preBotzinger complex depend on a calcium-activated non-specific cation current linked to glutamate receptors in neonatal mice. *J. Physiol.*, **582**: 113-125, 2007.

Pace R.W. and Del Negro C.A. AMPA and metabotropic glutamate receptors cooperatively generate inspiratory-like depolarization in mouse respiratory neurons in vitro. *Eur. J. Neurosci.*, **28**: 2434-2442, 2008.

Parkis M.A., Bayliss D.A., Berger A.J. Actions of norepinephrine on rat hypoglossal motoneurons. *J. Neurophysiol.*, **74**: 1911-1919, 1995.

Parkis M.A. and Berger A.J. Clonidine reduces hyperpolarization-activated inward current (Ih) in rat hypoglossal motoneurons. *Brain Res.*, **769**: 108-118, 1997.

Pearson J., Goldstein M., Markey K., Brandeis L. Human brainstem catecholamine neuronal anatomy as indicated by immunocytochemistry with antibodies to tyrosine hydroxylase. *Neuroscience*, **8**: 3-32, 1983.

Powers R.K. and Binder M.D. Persistent sodium and calcium currents in rat hypoglossal motoneurons. *J. Neurophysiol.*, **89**: 615-624, 2003.

Rainbow T.C., Parsons B., Wolfe B.B. Quantitative autoradiography of beta 1- and beta 2-adrenergic receptors in rat brain. *Proc. Natl. Acad. Sci. USA.*, **81**: 1585-1589, 1984.

Rajaofetra N., Poulat P., Marlier L., Geffard M., Privat A. Pre- and postnatal development of noradrenergic projections to the rat spinal cord: an immunocytochemical study. *Brain Res. Dev. Brain Res.*, **67**: 237-246, 1992.

Reiner P.B. Correlational analysis of central noradrenergic neuronal activity and sympathetic tone in behaving cats. *Brain Res.*, **378**: 86-96, 1986.

Rekling J.C., Funk G.D., Bayliss D.A., Dong X.W., Feldman J.L. Synaptic control of motoneuronal excitability. *Physiol. Rev.*, **80**: 767-852, 2000.

Remmers J.E., Degroot W.J., Sauerland E.K., Anch A.M. Pathogenesis of upper airway occlusion during sleep. *J. Appl. Physiol.*, **44**: 931-938, 1978.

Robinson D.M., Peebles K.C., Kwok H., Adams B.M., Clarke L.L., Woollard G.A., Funk G.D. Prenatal nicotine exposure increases apnoea and reduces nicotinic potentiation of hypoglossal inspiratory output in mice. *J. Physiol.*, **538**: 957-973, 2002.

Rosin D.L., Talley E.M., Lee A., Stornetta R.L., Gaylinn B.D., Guyenet P.G., Lynch K.R. Distribution of alpha 2C-adrenergic receptor-like immunoreactivity in the rat central nervous system. *J. Comp. Neurol.*, **372**: 135-165, 1996.

Roux J.C., Mamet J., Perrin D., Peyronnet J., Royer C., Cottet-Emard J.M., Pequignot J.M., Dalmaz Y. Neurochemical development of the brainstem catecholaminergic cell groups in rat. *J. Neural. Transm.*, **110**: 51-65, 2003.

Rukhadze I., Fenik V.B., Branconi J.L., Kubin L. Fos expression in pontomedullary catecholaminergic cells following rapid eye movement sleep-like episodes elicited by pontine carbachol in urethane-anesthetized rats. *Neuroscience*, **152**: 208-222, 2007a.

Rukhadze I. and Kubin L. Differential pontomedullary catecholaminergic projections to hypoglossal motor nucleus and viscerosensory nucleus of the solitary tract. *J. Chem. Neuroanat.*, **33**: 23-33, 2007b.

Rukhadze I., Fenik V.B., Benincasa K.E., Price A., Kubin L. Chronic intermittent hypoxia alters density of aminergic terminals and receptors in the hypoglossal motor nucleus. *Am. J. Respir. Crit. Care Med.*, **182**: 1321-1329, 2010.

Sauerland E.K. and Harper R.M. The human tongue during sleep: electromyographic activity of the genioglossus muscle. *Exp. Neurol.*, **51**: 160-170, 1976.

Sawaguchi T., Ozawa Y., Patricia F., Kadhim H., Groswasser J., Sottiaux M., Takashima S., Nishida H., Kahn A. Catecholaminergic neurons in the brain-stem and sleep apnea in SIDS victims. *Early Hum. Dev.*, **75** Suppl: S41-50, 2003.

Selvaratnam S.R., Parkis M.A., Funk G.D. Developmental modulation of mouse hypoglossal nerve inspiratory output in vitro by noradrenergic receptor agonists. *Brain Res.*, **805**: 104-115, 1998.

Sforza E., Haba-Rubio J., De Bilbao F., Rochat T., Ibanez V. Performance vigilance task and sleepiness in patients with sleep-disordered breathing. *Eur. Respir. J.*, **24**: 279-285, 2004.

Singer J.H., Bellingham M.C., Berger A.J. Presynaptic inhibition of glutamatergic synaptic transmission to rat motoneurons by serotonin. *J. Neurophysiol.*, **76**: 799-807, 1996.

Skydsgaard M. and Hounsgaard J. Spatial integration of local transmitter responses in motoneurones of the turtle spinal cord in vitro. *J. Physiol.*, **479**: 233-246, 1994.

Smeets W.J. and Gonzalez A. Catecholamine systems in the brain of vertebrates: new perspectives through a comparative approach. *Brain Res. Brain Res. Rev.*, **33**: 308-379, 2000.

Soja P.J., Morales F.R., Baranyi A., Chase M.H. Effect of inhibitory amino acid antagonists on IPSPs induced in lumbar motoneurons upon stimulation of the nucleus reticularis gigantocellularis during active sleep. *Brain Res.*, **423**: 353-358, 1987.

Soja P.J., Lopez-Rodriguez F., Morales F.R., Chase M.H. The postsynaptic inhibitory control of lumbar motoneurons during the atonia of active sleep: effect of strychnine on motoneuron properties. *J. Neurosci.*, **11**: 2804-2811, 1991.

Sokoloff A.J. and Deacon T.W. Musculotopic organization of the hypoglossal nucleus in the cynomolgus monkey, Macaca fascicularis. *J. Comp. Neurol.*, **324**: 81-93, 1992.

Sokoloff A.J. Topographic segregation of genioglossus motoneurons in the neonatal rat. *Neurosci. Lett.*, **155**: 102-106, 1993.

Sood S., Morrison J.L., Liu H., Horner R.L. Role of endogenous serotonin in modulating genioglossus muscle activity in awake and sleeping rats. *Am. J. Respir. Crit. Care Med.*, **172**: 1338-1347, 2005.

Sood S., Liu X., Liu H., Horner R.L. Genioglossus muscle activity and serotonergic modulation of hypoglossal motor output in obese Zucker rats. *J. Appl. Physiol.*, **102**: 2240-2250, 2007.

Specht L.A., Pickel V.M., Joh T.H., Reis D.J. Light-microscopic immunocytochemical localization of tyrosine hydroxylase in prenatal rat brain. I. Early ontogeny. *J. Comp. Neurol.*, **199**: 233-253, 1981a.

Specht L.A., Pickel V.M., Joh T.H., Reis D.J. Light-microscopic immunocytochemical localization of tyrosine hydroxylase in prenatal rat brain. II. Late ontogeny. *J. Comp. Neurol.*, **199**: 255-276, 1981b.

Steriade M., Datta S., Pare D., Oakson G., Curro Dossi R.C. Neuronal activities in brain-stem cholinergic nuclei related to tonic activation processes in thalamocortical systems. *J. Neurosci.*, **10**: 2541-2559, 1990.

Tadjalli A., Duffin J., Peever J. Identification of a novel form of noradrenergic-dependent respiratory motor plasticity triggered by vagal feedback. *J. Neurosci.*, 30: 16886-16895, 2010a.

Tadjalli A. and Peever J. Sleep loss reduces respiratory motor plasticity. *Adv. Exp. Med. Biol.*, **669**: 289-292, 2010b.

Talley E.M., Rosin D.L., Lee A., Guyenet P.G., Lynch K.R. Distribution of alpha 2A-adrenergic receptor-like immunoreactivity in the rat central nervous system. *J. Comp. Neurol.*, **372**: 111-134, 1996.

Talley E.M., Lei Q., Sirois J.E., Bayliss D.A. TASK-1, a two-pore domain K^+ channel, is modulated by multiple neurotransmitters in motoneurons. *Neuron*, **25**: 399-410, 2000.

Tohyama M., Wanaka A., Araki T., Betz H., Malbon C.C. Localization of glycine and beta-adrenergic receptors in the rat brain. *Arch. Histol. Cytol.*, **52**: 39-48, 1989.

Veasey S.C., Zhan G., Fenik P., Pratico D. Long-term intermittent hypoxia: reduced excitatory hypoglossal nerve output. *Am. J. Respir. Crit. Care Med.*, **170**: 665-672, 2004.

Viana F., Bayliss D.A., Berger A.J. Multiple potassium conductances and their role in action potential repolarization and repetitive firing behavior of neonatal rat hypoglossal motoneurons. *J. Neurophysiol.*, **69**: 2150-2163, 1993.

Viana F., Bayliss D.A., Berger A.J. Postnatal changes in rat hypoglossal motoneuron membrane properties. *Neuroscience*, **59**: 131-148, 1994.

Viana F., Bayliss D.A., Berger A.J. Repetitive firing properties of developing rat brainstem motoneurones. *J. Physiol.*, **486**: 745-761, 1995.

Viemari J.C., Maussion G., Bevengut M., Burnet H., Pequignot J.M., Nepote V., Pachnis V., Simonneau M., Hilaire G. Ret deficiency in mice impairs the development of A5 and A6 neurons and the functional maturation of the respiratory rhythm. *Eur. J. Neurosci.*, **22**: 2403-2412, 2005.

Volgin D.V., Mackiewicz M., Kubin L. Alpha1B receptors are the main postsynaptic mediators of adrenergic excitation in brainstem motoneurons, a single-cell RT-PCR study. *J. Chem. Neuroanat.*, **22**: 157-166, 2001.

Walton K. and Fulton B.P. Ionic mechanisms underlying the firing properties of rat neonatal motoneurons studied in vitro. *Neuroscience*, **19**: 669-683, 1986.

Weinberg D.H., Trivedi P., Tan C.P., Mitra S., Perkins-Barrow A., Borkowski D., Strader C.D., Bayne M. Cloning, expression and characterization of human alpha adrenergic receptors alpha 1a, alpha 1b and alpha 1c. *Biochem. Biophys. Res. Commun.*, **201**: 1296-1304, 1994.

Wilkerson J.E. and Mitchell G.S. Daily intermittent hypoxia augments spinal BDNF levels, ERK phosphorylation and respiratory long-term facilitation. *Exp. Neurol.*, **217**: 116-123, 2009.

Wise A., Lee T.W., MacEwan D.J., Milligan G. Degradation of G11 alpha/Gq alpha is accelerated by agonist occupancy of alpha 1A/D, alpha 1B, and alpha 1C adrenergic receptors. *J. Biol. Chem.*, **270**: 17196-17203, 1995.

Wu D., Katz A., Lee C.H., Simon M.I. Activation of phospholipase C by alpha 1-adrenergic receptors is mediated by the alpha subunits of Gq family. *J. Biol. Chem.*, **267**: 25798-25802, 1992.

Yamuy J., Fung S.J., Xi M., Morales F.R., Chase M.H. Hypoglossal motoneurons are postsynaptically inhibited during carbachol-induced rapid eye movement sleep. *Neuroscience*, **94**: 11-15, 1999.

Yasuda K., Robinson D.M., Walsh C.W., Selvaratnam S.R., McMorland A.J.C., Funk G.D. Modulation of hypoglossal motoneuron activity by SP in neonatal mice in vitro: cellular and synaptic mechanisms. *J. Physiol.*, **534**: 447-464, 2001.

Yasuda K., Nakayama Y., Tanaka M., Mori R., Furusawa K. The distribution of respiration-related and swallowing-related motoneurons innervating the rat genioglossus muscle. *Somatosens. Mot. Res.*, **19**: 30-35, 2002.

Zeng D.W., Harrison J.K., D'Angelo D.D., Barber C.M., Tucker A.L., Lu Z.H., Lynch K.R. Molecular characterization of a rat alpha 2B-adrenergic receptor. *Proc. Natl. Acad. Sci. USA.*, **87**: 3102-3106, 1990.

Zhan G., Serrano F., Fenik P., Hsu R., Kong L., Pratico D., Klann E., Veasey S.C. NADPH oxidase mediates hypersomnolence and brain oxidative injury in a murine model of sleep apnea. *Am. J. Respir. Crit. Care Med.*, **172**: 921-929, 2005.

Zhong H. and Minneman K.P. Alpha1-adrenoceptor subtypes. *Eur. J. Pharmacol.*, **375**: 261-276, 1999.

Zhu Y., Fenik P., Zhan G., Mazza E., Kelz M., Aston-Jones G., Veasey S.C. Selective loss of catecholaminergic wake active neurons in a murine sleep apnea model. *J. Neurosci.*, **27**: 10060-10071, 2007.